O. Bilohub, Yu. Gusev, F. Sirenko

CONNECTING RODS, CRANKSHAFTS, CYLINDERS AND CYLINDER BLOCKS OF AIRCRAFT PISTON ENGINES

2017

MINISTRY OF EDUCATION AND SCIENCE OF UKRAINE
National aerospace university
«Kharkiv aviation institute»

O. Bilohub, Yu. Gusev, F. Sirenko

CONNECTING RODS, CRANKSHAFTS, CYLINDERS AND CYLINDER BLOCKS OF AIRCRAFT PISTON ENGINES

Manual

Kharkiv «KhAI», 2017

UDC 621.432:621.824.32.001.24 (075.8)
BBL 31365я73
B 58

Розглянуто матеріали, з яких виготовлено елементи технологій виробництва і розрахунки на міцність елементів, що входять до складу конструкцій.

Для студентів спеціальності «Авіаційні двигуни і енергетичні установки» при виконанні лабораторних робіт, а також курсових і дипломних проектів.

Reviewers: Doctor of technical sciences, professor V. Pylov,
Candidate of technical sciences, Associate Prof. V. Korogodsky

Bilohub, O.

B 58 Connecting rods, crankshafts, cylinders and cylinder blocks of aircraft piston engines [Text] : manual / O. Bilohub, Yu. Gusev, F. Sirenko. – Kharkiv : National aerospace university «Kharkiv aviation institute», 2017. – 76 p.

ISBN 978-966-662-534-5

The manual considers the construction of connecting rods, crankshafts, cylinders and cylinder blocks of the aircraft piston engines. The manual also contains the information about the materials, of which piston engines are made, and the strength analysis of the elements.

This manual will be interesting for the students studying “Aircraft engines and power plants” at laboratory activities, term works, and master thesis.

Figures. 51. Tables. 3. References.: 7 items

UDC 621.432:621.824.32.001.24 (075.8)
BBL 31365я73

ISBN 978-966-662-534-5

CONTENTS

1 BASIC FACTS ABOUT CONSTRUCTION AND OPERATION

Connecting rod is an engine element connecting a crankshaft and a reciprocating piston. For that reason, it bears and delivers to the crankshaft all the loads from the reciprocating piston. Hence, it operates itself alternately, changing from compressed to tensed state and back. The extreme compression corresponds to the moment of the maximum gas pressure in a cylinder, and the extreme tension can be observed when the piston gets to the top dead center at the beginning of the intake stroke. In the latest moment, the inertia acting the piston becomes maximal; it acts upwards.

A compound motion of the connecting rod can be considered as consisting of two simple motions: reciprocation together with the piston and hobbing around the piston pin axis. The hobbing happens because of accelerations in the hobbing plane. They initiate an inertia, which bends the connecting rod. The inertia is negligibly small, so it is usually neglected in a strength analysis.

The following three elements can be distinguished in the connecting rod:

a) a small end (connects the piston pin with the connecting rod);

b) a big end (connects the crankshaft with the connecting rod);

c) a web (connects the small end with the big end).

The generic scheme of the connecting rod with a detachable big end is shown in *Figure 1*.

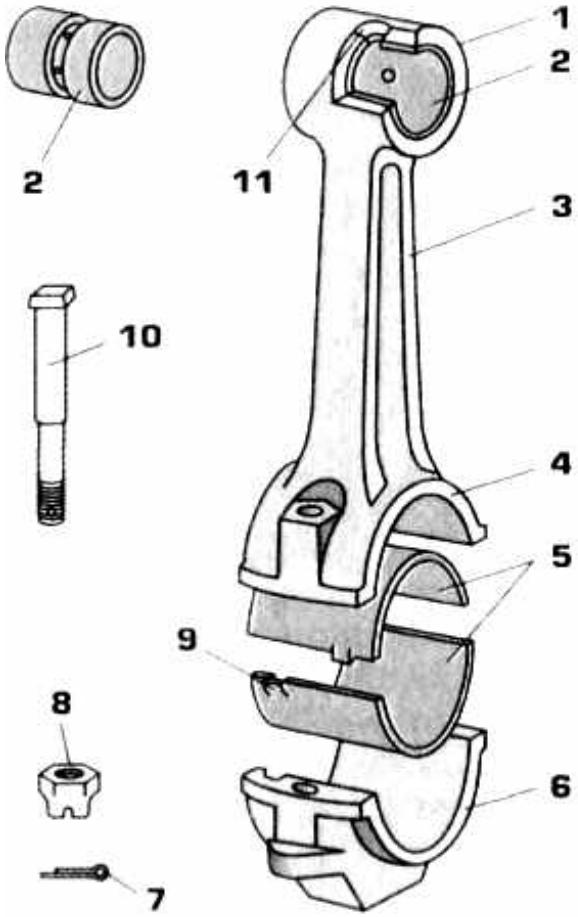

Figure 1 – The generic connecting rod with a detachable big end: 1 – small end; 2 – small end bearing; 3 – web; 4 – big end upper half; 5 – big end bearing; 6 – big end lower half; 7 – split pin; 8 – castell nut; 9 – nib of the big end bearing; 10 – locking bolt

The distance between the big and small ends is termed *length of the connecting rod (l).* The following features determine the length:

– a wall force N (the force acting through the piston on the cylinder wall) decreases with the increase of the connecting rod (or in the other words with the decrease of $\lambda = R/l$, where R is a throw);

– the minimum length must provide the free connecting rod passing

near the crankshaft elements in the BDC and the cylinder barrel at the maximum hobbing angle.

The second feature is decisive for modern engines. Therefore the connecting rod is tried hard to be the minimum-length, but at the same time, it must meet the free motion demand (the web and the big end must move freely in the cylinder).

The corresponding λ ratio may vary within the range 1/3.7…1/4.2 for a star engines and within the range 1/3.2…1/3.7 for a V-shape engine.

Engines with a single crank reciprocating some pistons may have their connecting rods arranged centrally or adjoin.

In the case of adjoin arrangement, the piston of a single cylinder is connected to a crankpin journal by means of a master connecting rod. The rest pistons are connected to the big end of the master connecting rod by means of link rods.

The star engines have their connecting rods arranged adjoin. The V-shape engines with two pistons actuated by a single crank may have their connecting rods arranged both centrally and adjoin. Each arrangement has its own advantages and disadvantages. Let us consider the main ones.

The big end of the master connecting rod is very rigid. Hence, it strains insignificantly despite the big number of the connected link rods (especially essential for the star engines). The disadvantage of the adjoin arranged connecting rods is the different piston kinematics in different cylinders and additional forces from the link rods acting the master connecting rod and its piston. In the case of the centrally arranged connecting rods, the kinematics of all pistons is similar. The big end then is also loaded more uniform, which is a great piece of news for the bearing inside the big end. The disadvantages of the central connecting rod arrangement are low rigidity of the big end and the problems in placing more than two connecting rods on a single crankpin journal. The just mentioned disadvantages make the centrally arranged connecting rods suite only for the V-shape engines. Besides, there may appear the problems with a limited bearing surface of the connecting rod bearing.

In order to reduce the wear out of the friction surfaces of the piston pin and the connecting rod, a bush made of an antifriction material is pressed in the small end. The piston pin–connecting rod assembly is lubricated with oil sprayed at high pressure or with oil splashed by the fast moving parts of the crank rod assembly. In the first case (see *Figure 10*) the oil for the small end is delivered from the big end. There it gets from the inside of the crankshaft through the special pipe that is pinned to the web, or through the channel inside the web. Finally oil from the channel or from the pipe gets to the clearance between the friction surfaces.

In the second case, the oil droplets get on the friction surfaces of the bushed piston pin bearing and the piston pin through the special holes in the small end (see *Figure 9*).

The big end of the link rod is pinned to the big end of the master connecting rod. The pin is rigidly clamped in the web.

The link rod pin is shorter than the piston pin. The shorter pin turns into a lower bending moment and, as the result, into a smaller pin diameter is.

The small pin size and its fixation in the connecting rod cause high specific pressure on the friction surface between the pin and a big end of the link rod. The oil delivered at high pressure lubricates the just mentioned friction pair minimizing its wear out.

The big end of the master connecting rod can be produced all-in-one (see *Figure 11*) or detachable (see *Figure 2*). If the connecting rod is all-in-one, then the crankshaft must be detachable; and inversely, if the crankshaft is a single-piece part, then the connecting rods must be detachable.

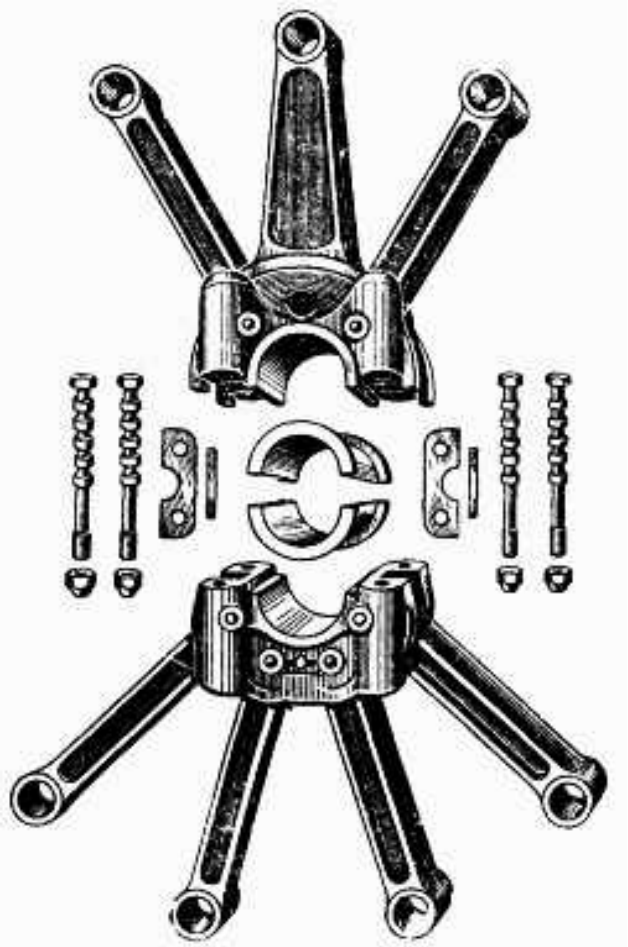

Figure 2 – Master connecting rod of the star engine with the detachable big end

If the crankshaft is all-in-one, then the big end of the non-detachable connecting rod can rest only on the roller bearings (see *Figure 3*).

The connecting rod, in this case, is put on the crankshaft`s end and is drawn over the specially cut webs (for example, connecting rods of BMW-6 V-shape engine).

Usually, the three-, four- or six-crank crankshafts of the V-shape and in-line engines are all-in-one, therefore the big end of the connecting rod is detachable. To downsize the connecting rod, the split of the big end is tilted to the web axis.

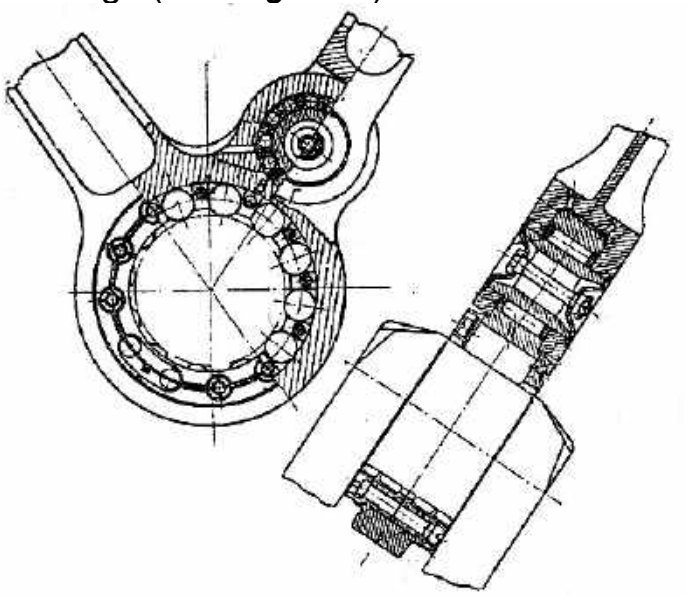

Figure 3 – Non-detachable big end of the master connecting rod with the roller bearing

Opposite to the just discussed engine types, the connecting rods of the star engines are mostly single piece and the crankshaft is detachable. Such a design is caused by the problems that appear when designers try to develop the split of the big end of the master connecting rod (especially in the case of numerous link rods). And inversely, if a number of cranks is low, then the development of the detachable master connecting rod turns to an easy task for the designers.

Sometimes, following the objectives of a simple crankshaft construction and its high rigidity, the master connecting rod of a star engine has its big end detachable (see *Figure 2*). The fastening elements of the detachable joint make the big end heavier, increasing the inertia of the rotating mass in that way. The inertia loads the bearings of the connecting rod and limits an engine speed up. Hence, the application of detachable big end connecting rod is appropriate only for multi-star engines, where the detachable shaft is unacceptable.

The big end lower half is lock-bolted or lock-studded to the connecting rod (see *Figure 3* and *7*). In the second case, the mass and overall sizes of the big end go down, but then the misalignment of stud axes in relation to the face surface of the big end lower half becomes more complex problem than the misalignment of the bolt axes.

The VK-105 (see next) has a unique joint of the big end lower half and the web. The precise positioning of the big end lower half is provided by special locks or grooves (see *Figure 3, b, c*) or by centering spigots of the tightening bolts (*Figure 4, a*).

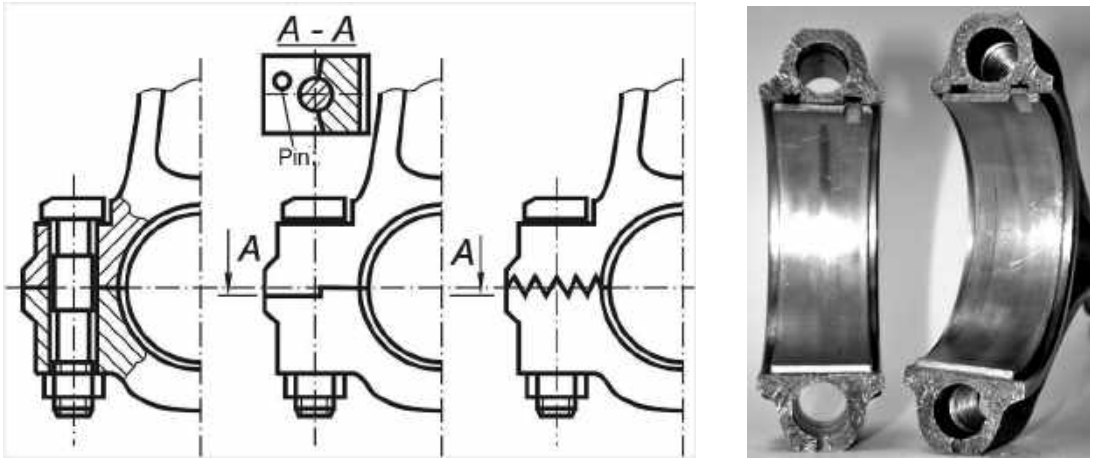

a b c d

Figure 4 – The fixation of the big end lower half with: a – precise bolts; b – cylindrical spigots; c – face splines; d – “split” joint

When the face splines are used, the joint is additionally equipped with a pin. It performs the axial fixation and constrains the big end lower half from the angular shift against the web. *Figure 3*, d presents the “split” fixation. The split appears while the big end lower half is broken off.

2 BEARINGS

Reliable and time proof bearing must fulfill the requirements presented below.

Antiscoring resistance is a bearing`s ability to avoid the seizing of a bearing in the case of oil shortage. The material of the bearing must:

- adsorb and firmly keep the oil film on the bearing surface;
- have high thermal conductivity and heat capacity;
- not be tended to a seizure, i.e. must not be tended to metal contact formation (if the contact is formed, then it must be destroyed very quickly; the low melting temperature and low shear strength can assist with this phenomenon).

Conformability is a bearing ability to shape itself (neck shape) because of the own wear out and plastic straining. The high-conformable materials are usually of low rigidity and have low elasticity modulus.

Friction coefficient. The friction coefficient plays a great role when selecting material for bearings. It should not be forgotten that the total friction losses are also considerably affected by the finish of a friction surface, the oil quality, and its pressure. The sliding speed and ability to absorb and firmly keep the oil film on the bearing surface also do matter.

Wear resistance of the bearings and the crankshaft. Soft materials, like lead-based alloys, fit the slide bearing the most because of more rigid materials, like copper-lead alloys, require more fair oil filtration from the solid and abrasive particles.

Plastic resistance. The bearing must have compression strength enough at the temperature 150 °C.

Fatigue strength. The fatigue appears because of thermal fatigue, which in its turn is caused by a cyclic temperature alternation.

Corrosion resistance. Corrosion intensifies the wear out and reduces the antifriction properties of the bearing. This considerably increases the chance of the fins. Hence, the used material must have the high corrosion resistance when working in the blown oil at high temperature.

The crankpin bearing is among the most loaded and responsible engine parts. It considerably limits the engine speed-up (it is more essential for star engines) because of the high loads and high slippage speed of the big end against the crankpin journal. The mentioned loads alternate both by the magnitude and by direction. The vector diagrams of forces acting on the crankpin journal are shown in *Figure 5*.

The operability of the bearing at the definite load depends on its sizes (diameter and area of friction surfaces), material (see chapter 4), finishing of the friction surfaces and lubrication conditions. Ceteris paribus, the bigger bearing, the less specific pressure acts on the bearing resulting in a lesser wear out. But unfortunately, the sizes of the bearings are determined by the crankshaft construction and are limited by its overall sizes and weight.

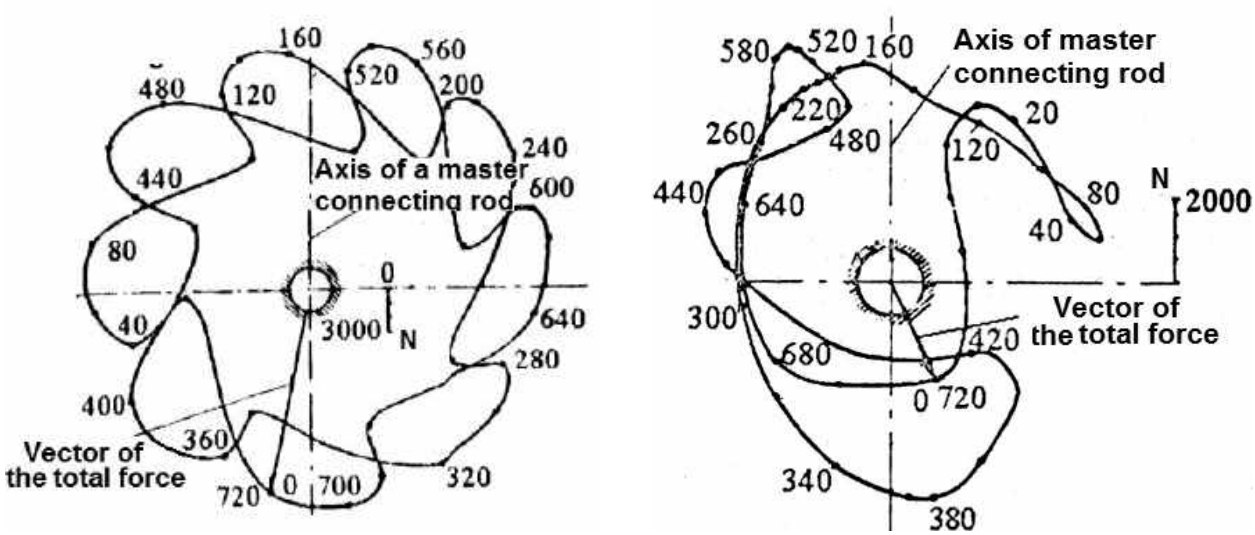

Figure 5 – Vector diagram of forces that act on the big end bearing:
a – star nine-cylinder engine; b – twelve cylinder V-shape engine
(digits correspond to a crank angle within the range 0…720)

The connecting rod with the detachable big end has its bearing consisting of two bearing halves. If the connecting rod has a non-detachable big end, the bearing is designed single piece. It looks like a thin-wall cylindrical cartridge the so-called bush. Most connecting rods with the non-detachable big end have the bearing pressed inside. Besides, the bearing is stopped to avoid the shift. The friction in the bearing happens between the crank and the internal surface of the big end.

The above-mentioned properties are easy to fulfill by following these constructive recommendations:

– the surface of the crankshaft must have a high hardness (Brinell hardness number must be greater than 360-390 for the uncemented and non-nitrogenized shafts, 590…610 for the cemented and nitrogenized shafts);

– the friction surface of the bearing must be coated with a soft metal (2–20 μm), like lead, tin, indium or them-based composites to improve the run-in of the bearing on the crankshaft of the star engine;

– the scavenged oil must be filtered better to remove the debris.

The oil layer gets thinner while the load acting on the bearing grows. The maximum load that retains the extreme-thin, but continuous oil layer between the bearing and the shaft is determined by the bearing capacity.

As you may know, the maximum bearing capacity corresponds to the thinnest permissible oil layer. From this point of view, the finish of the friction surfaces makes a considerable effect on the bearing capacity and reliability of the bearing. In our particular case, this is topical for a friction pair “big end bearing – crankpin journal”.

The thickness of the oil layer in the most loaded patches may be some microns. So, their finish and the precision of their shape must be extremely high to avoid the boundary friction.

To provide the sufficient bearing capacity, the bearing must have no oil draining grooves, holes or recesses at the heavily loaded patches. The star engines have their bearings pressed in the connecting rod. Hence their entire working surface is heavily loaded (see *Figure 5, a*). Considering all above mentioned, it is obvious that the working surface must be smooth, without any grooves or drillings. Even the bearing fixation in the connecting rod is made by face splines. (*Figure 12*).

The big end bearings of the V-shape engines are heavily loaded too. But opposite to the star engines their working surface has heavily loaded patches and less loaded patches (see *Figure 5, b*). Sometimes the less loaded patches have grooves, which facilitate the oil distribution over the entire working surface. Engines of the past had the floating bearings which were loosely fitted in the counterbore of the big end (*Figure 6*).

In this case, the work done by the friction forces is shared between two working surfaces. Nowadays this construction is interesting only in a historical context.

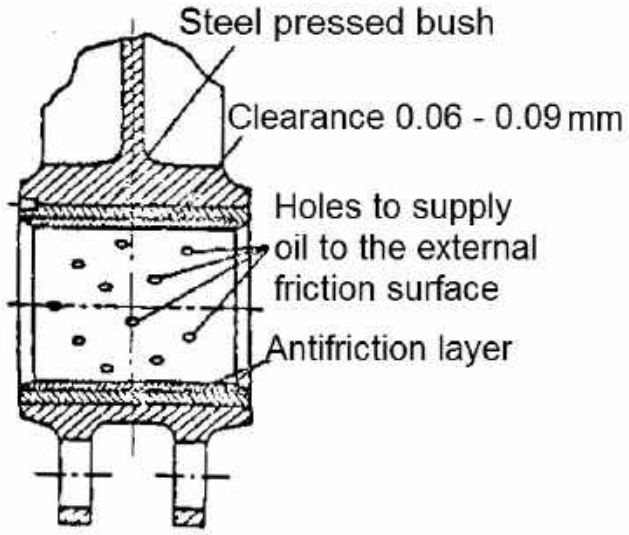

Figure 6 – The big end with the floating bearing

The operation of the big end bearing becomes harder when the axes of the crankpin journal and the big end are misaligned. In the most cases, the misalignment tends to the jamming of the bearing ends on the crankpin journal. To prevent this, the counterbore is made conical, expanding to the sides of the big end.

Sometimes, the misalignment can be eliminated by the free fit (the clearance is 0.03-0.07 mm) of the bearing in the big end. In this case, having been acted by the forces, the bearing can self-center on the crankpin journal. The bearing cannot turn against the big end because they are joined by the face splines.

Sometimes, the end clearances between the friction surfaces of the bearing and the connecting rod (see *Figure 11*) are sealed to enhance the bearing capacity. In this case, the pressure in the oil layer grows higher along the entire length of the bearing. This is especially important at the ends. Besides, such seal allows creating a volume at the end of the bearing surface to feed the oil for the pins of link rods and their bushes lubrication. But this construction has the profit only for the connecting rods of the star engines because of the following reasons:

– the construction with end seals becomes more complex;

– it is a great challenge to seal the big end when the bearings are split.

The single piece bearings of the star engines are usually thin-wall (the width is 2-3 mm) because thick walls increase the weight and the overall sizes of the big end. The detachable bearings of the in-line and V-shape engines can be both thin-wall (1.5 – 2.5 mm) and thick-wall (5 – 9 mm). The thick-wall bearings found their use for the master rods.

The finishing of the inner bearing`s surface happens after it has been pressed in the connecting rod. Sometimes, the bearing is pressed by the special tool, which eliminates the deformations of the bearing while pressing. The fragment of the drawing of the bearing insert is shown in *Figure 7*. There one may find the requirements to the precision and quality of the surface. The construction of the thin-wall bearing of the automotive engine is shown in *Figure 8*.

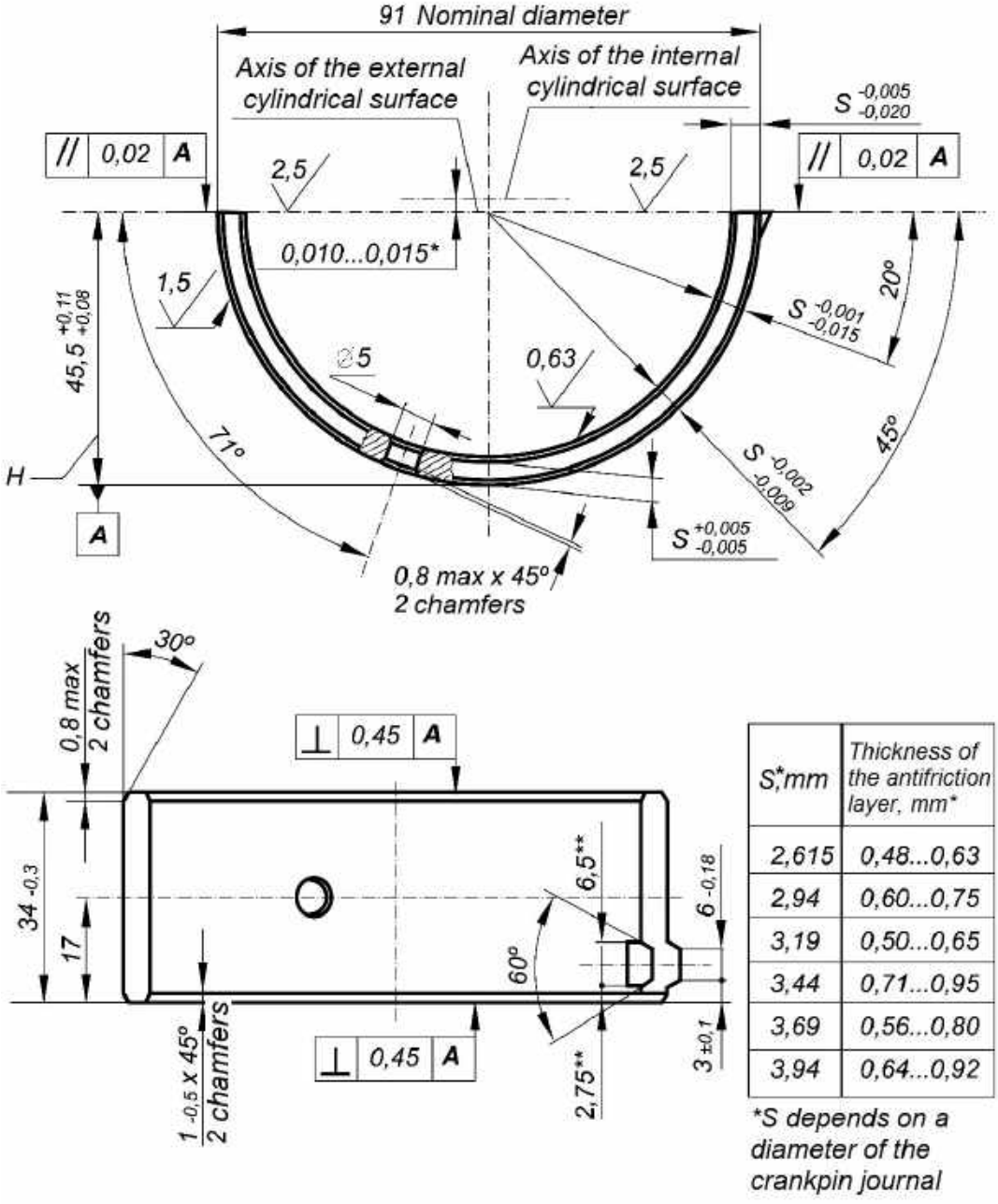

Figure 7 – Fragment of the drawing of the crankpin bearing insert

The usage of the ball or roller bearings is associated with the considerable increase of weight and overall sizes of the big end, which in its turn becomes the reason for greater inertia and bigger overall sizes of the crankcase and an engine as a whole. The crankcase must be big enough to let the connecting freely move in the crankcase and near the bottom sides of the cylinder barrels.

For the above-mentioned reasons, the roller bearings are not used in the modern engines. The only one exception is the high-speed small-displacement two-stroke engines. The friction surfaces are lubricated with oil that is a component of air/gasoline/oil mixture.

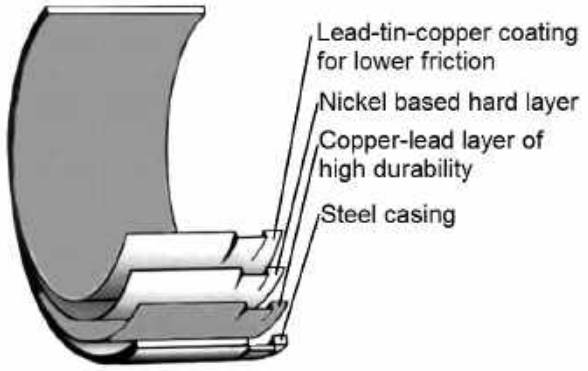

Figure 8 – Construction of the modern thin-wall multilayer bearing

3 EXAMPLES OF CONNECTING RODS

3.1 Connecting rods of the AM-38 piston engine.

The AM-38 piston engine (*Figure 9*) has its connecting rods arranged adjoin. Both master and link connecting rods are forged from the chrome-nickel steel. The small ends of both connecting rods have the bronze bushes pressed inside. Each bush is constrained from a turning by the stop pin. The small end and its bronze bush have few apertures to lubricate the friction surfaces of the piston pin and the bush with oil. The oil is splashed because of crankshaft rotation. The web of the master connecting rod has the I-beam shape. The distance between the flanges of the I-beam grows from the big end to the low end. The big end has the split tilted at an angle 60° to the connecting rod axis. The pin of the link connecting rod is fitted in the eye of the master connecting rod. The eye is tilted at the angle 67° to the connecting rod axis. Such position of the eye reduces the load acting on the master rod from the link rods. The big end lower half is attached to the web by six studs. It has four ribs for higher rigidity. The fixation of the lower half is made by the annular ledge in the both split faces of the parts. The bearing consists of two components, each of which is constrained in the corresponding half of the big end by the locking device.

The web of the link rod has an I-beam shape. The I-beam section remains constant along the connecting rod. The big end of the link rod has the shape of the fork that encompasses the eye of the master connecting rod. Both halves of the link rod big end have the bronze bearings pressed inside.

The pin is secured in the eye of the master connecting rod. It can freely hob in the bronze bearing of the link rod. The axial displacement of the pin is constrained by the special bolt, screwed in the eye of the master rod. The bolt

enters the milled-out pit on the pin surface.

The oil at high pressure is taken from the crankshaft to lubricate the friction surface of the bearing. It gets in the clearance between the pin and the bronze bearings through the drillings in the bearing, the big end, and the eye.

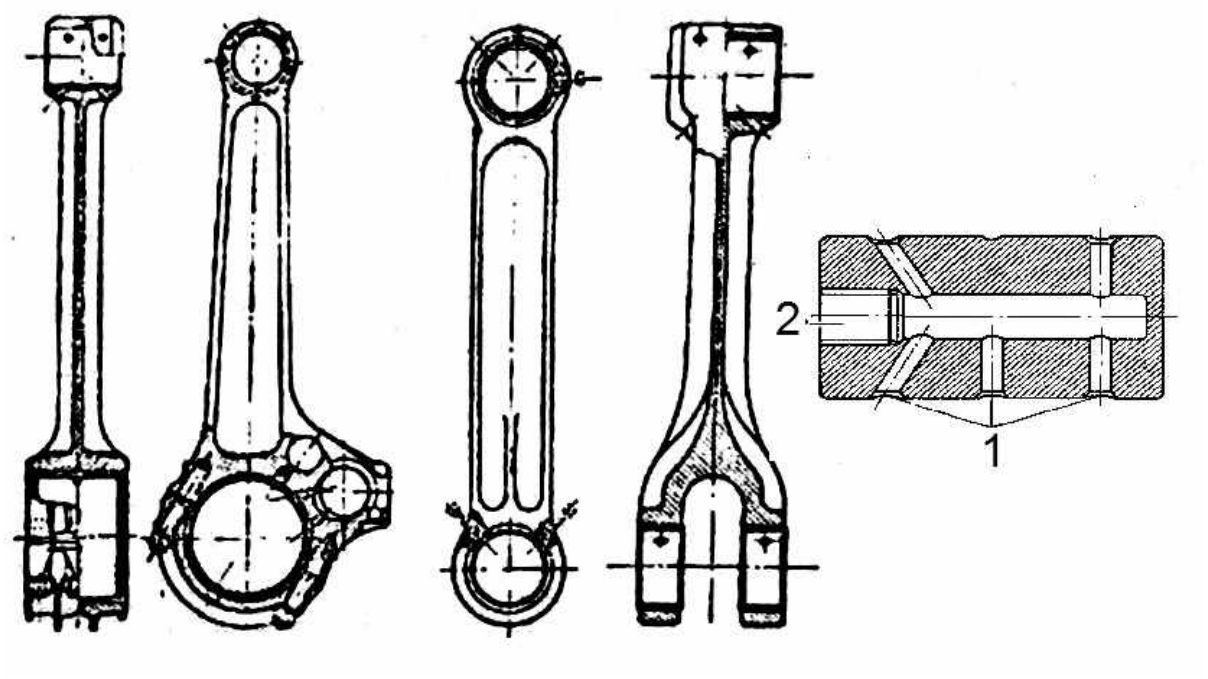

a b

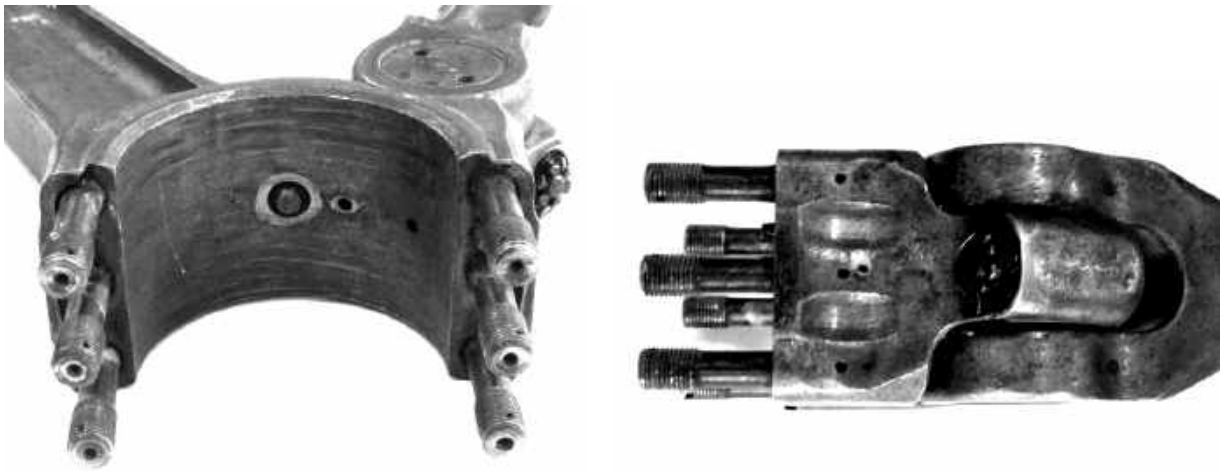

c d

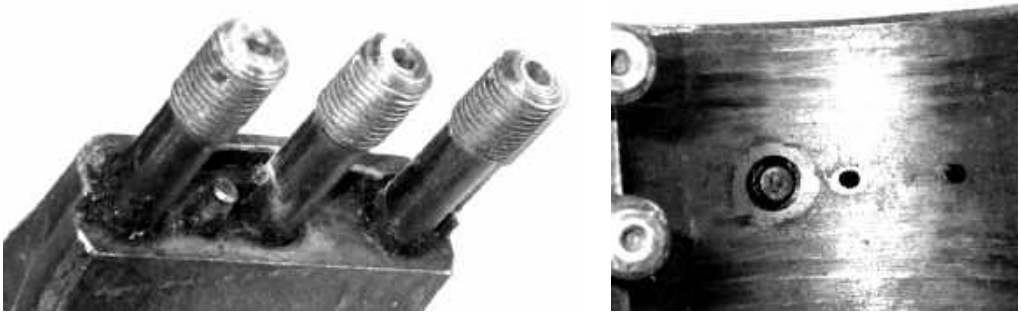

e f

Figure 9 – The connecting rods of the AM-38 V-shape engine: a – master connecting rod; b – link rod (1 – oil feeding channels, 2 – hole for the end cap); c – view from the lower half side; d – fixation of the link rod pin; e – centering elements (the ledge and the pin); f – locking device preventing the bearing from the turn.

3.2 Connecting rods of the VK-105 engine

The VK-105 engine (*Figure 10*) has its connecting rods arranged adjoin, but the pin angle is equal to the angle between the axes of the blocks. The master rod has an I-beam shape (*Figure 10, a*). The big end lower half is joined to the web by the special projections and grooves, which are milled on the split faces of parts. The projections have the conical holes to tightly press the conical pins. The pins take the shear loads in some sections simultaneously. Hence, the pins are of small diameter. The oil is supplied from the big end bearing to the piston pin through the pipe, riveted to the wall of the web. The construction of the link rod is presented in the *Figure 10, a*. The link rod is of the annular section with the cavity inside. The cavity is filled with oil during operation. The link rod is joined to the master connecting rod by the pin and the eye in the big end of the master connecting rod. The pin, joining connecting rods, suffers from the high bending moment. To cope with this problem it is equipped with the notch in the middle of the link rod`s big end (see *Figure 10, a*). The protuberance of the master connecting rod enters the notch (see *Figure 10, b*). It serves as an additional (middle) support of the pin, which considerably unloads the pin from bending.

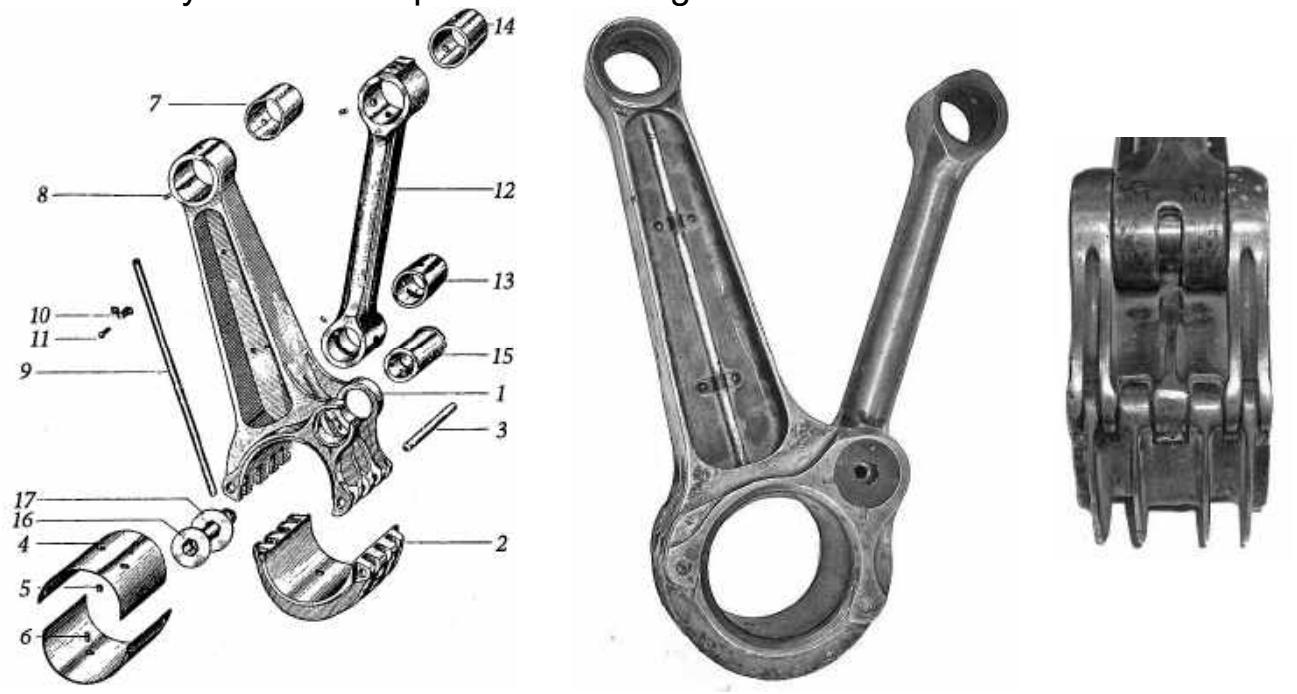

a b

Figure 10 – Connecting rods of the VK-105 engine:
a – master connecting rod and link connecting rod; b – picture of the connecting rod and the locking element; 1 – master connecting rod; 2 – lower half of the master connecting rod; 3 – conical pin; 4 – bearing of the bid end of the master connecting rod; 5, 6 – detent pin of the bearing; 7 – the bearing of the small end of the master connecting rod; 8 – detent pin of the small end of the master connecting rod; 9 – oil feeding pipe of the master connecting rod; 10, 11 – rivet and cramp to secure the oil feeding pump; 12 – link connecting rod; 13 – the bearing in the bid end of the link rod; 14 – the bearing in the small end of the link rod; 15 – pin of the small end of the link rod; 16 – plug;
17 – retaining washer of the plug

3.3 Centrally arranged connecting rods

The construction of the top head and the web of the centrally arranged connecting rods has no fundamental differences from that of the adjoin connecting rods (*Figure 11*). The big end of one connecting rod of each crank has the shape of the fork with a big notch in the center. There is a big end of the blade connecting rod inside the notch. The internal boring of the big end of the fork connecting rod has the rigidly fixed steel insert filled with an antifriction alloy from inside and outside.

Two halves of the fork connecting rod are bolted together (by two bolts). The lower half of the blade connecting rod is also bolted (2 bolts) to the web. But the bolts are bigger.

The lower halves of connecting rods are fixed to the big ends by the centering shoulders on the connecting bolts (engines Allison C-15, USA, Rolls-Royce «Merlin XX», Great Britain) or by the splines and the pins (engines DB-601, DB-605, Germany).

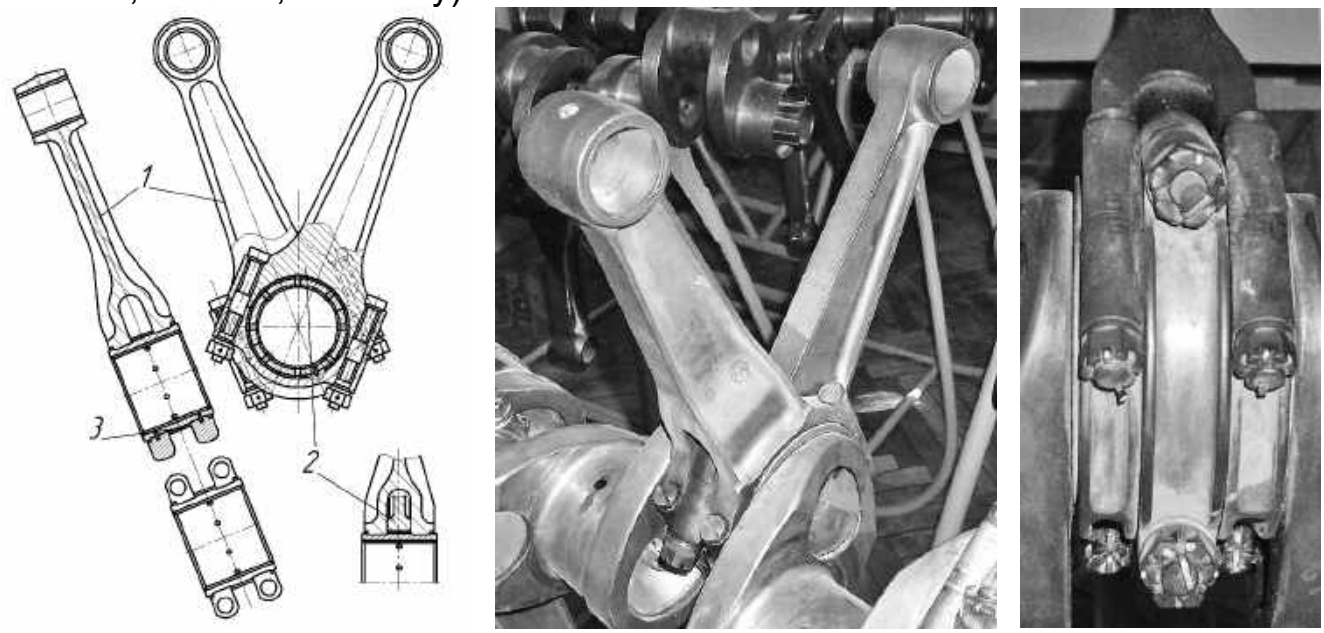

a b c

Figure 11 – The central connecting rods of the V-shape engine:
a – design scheme, b and c –connecting rods of Allison C-15.

The neighboring central connecting rods are the most used construction for the automotive V-shape engines nowadays. The left and right cylinder blocks of these engines are mutually shifted by the distance equal to the distance between the connecting rods. To keep the same bearing capacity of the bearings, the crankpin journal has higher length.

3.4 Connecting rods of a star engine

Let us consider the connecting rods of the two-row fourteen-cylinder engine ASh-82 (*Figure 12*). The connecting rod assembly consists of a single

master connecting rod and six link rods, which connecting pins are in the webs of the big end of the master connecting rod at equal angles $(\gamma = 51°25')$.

Like most of the star engines, the detachable crankshaft of ASh-82 lets the implementation of the all-in-one big end. The steel bush 4 (see *Figure 11*) is filled in with leaded bronze from inside. It is pressed in the big end of the connecting rod 5, which is stopped by the special locking device 3. It is put on the splines, which are splined on the face of the bearing 4. The locking device in its turn is bolted to the pins joining the link rods 8 with the master rod. The oil is supplied from inside of the crankshaft through the drillings in the big end. Next, it gets to the butt cavities of the bearing through the clearance between the bush and the crankshaft. The cavities are sealed with the oil-seal ring 1 and 10. From the cavity, oil gets to the special holes in the locking device 3 and next to the pins 8 of the link connecting rods. It lubricates the friction surfaces of the pins and the bronze bushes 9 that are pressed in the big ends of the link rods. As you may observe, the working surface of the bush is free from any drillings or grooves.

The oil-seal rings 1 and 10 are placed on both sides of the big end and sealed with the leaded bronze. There is a spring 2 between the front shim and the locking device. The spring presses the shim to the ends of the crankpin journal. The rings filled with the antifriction alloy reduce the friction and the wear out. It also prevents the oil leakage from the bearing volume.

Opposite to the most, the I-shape master connecting rod has flanges arranged parallel to its hobbing plane. This shape reduces the bending section modulus in the plane but makes the connecting rod much manufacturable. This is especially important in the sprawl, where the web changes to the big end. The pins are nitrogenized that considerably improves the hardness of the surface. The bushes pressed in the small and big ends of the link rods are thin-walled. They are made of the rolled bronze.

3.5 Connecting rod of the ROTAX-582 gasoline two-stroke two-cylinder engine

The connecting rod is a stamped part with the following machining (*Figure 12*). It has an I-beam shape. The big end is single-piece. The big and small ends of the connecting rods have the needle sleeve bearings. The inner surface of the big end bore and the external surface of the piston pin and crankpin journal are cemented.

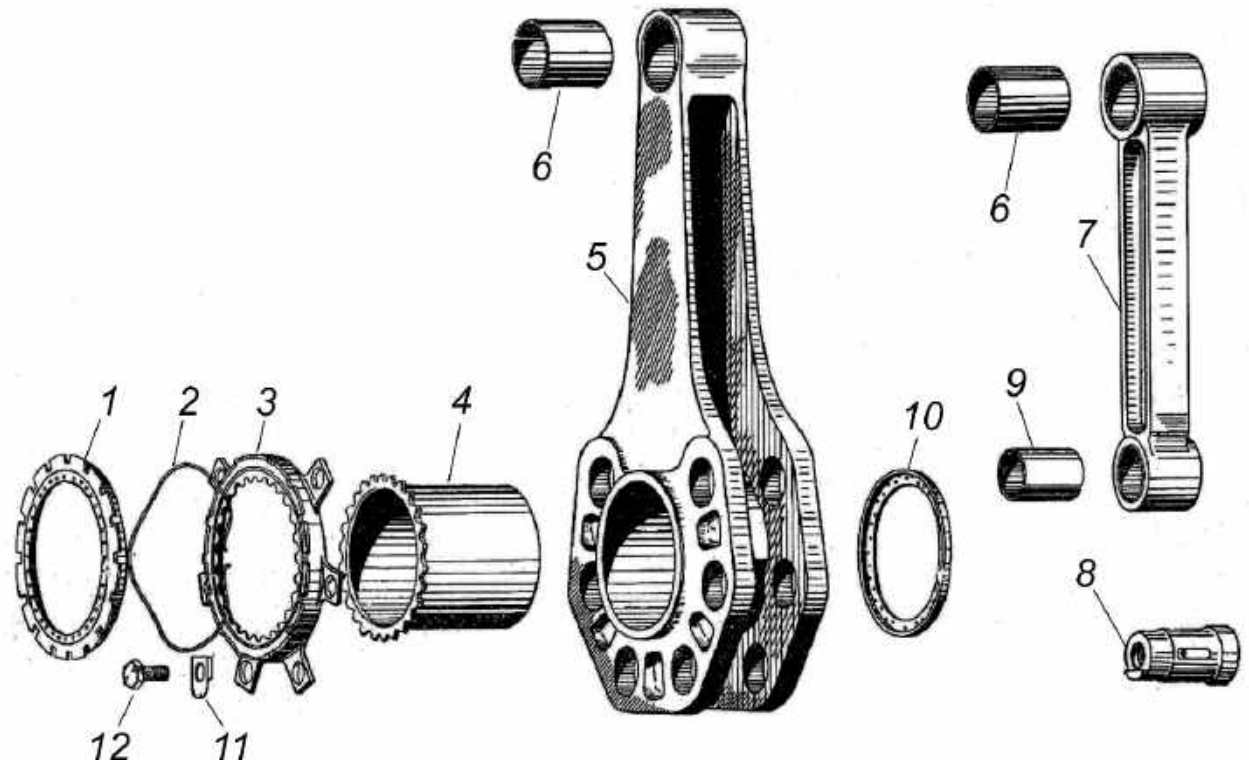

Figure 12 – Connecting rods of the ASh-82 star engine:
1 – front shim in the bush of the master connecting rod; 2 – spring;
3 – the locking device of the master connecting rod and pins of the link rods;
4 – bearing in the big end of the master connecting rod; 5 – master connecting rod;
6 – the bearing in the small end of the master connecting rod and link rods; 7 – link connecting rod; 8 – pin of the link connecting rod; 9 – bearing in the big end of the link rod;
10 – rear shim of the bush of the master connecting rod; 11 – stopper of a screw;
12 – screw that secures the stopper of the bush in the master connecting rod.

4 MATERIALS AND PRODUCTION

The connecting rods are usually forged or stamped.

The following are recommended steels for different connecting rods. The recommendations are the takeaway of the rich experience in production and maintenance of the different connecting rods:

– aircraft engines – steels ЭИ274 or 18НВА;

– automotive positive ignition engines – steels 40Г, 45Г2, 40Х, and 40ХН;

– automotive and tractor diesel engines – steels 18Х2Н4МА; 40ХН2МА; 40ХН3МА (the usage of the pearlite ductile cast iron is also possible);

– heavily loaded bulky connecting rods – steels 18Х2Н4МА, 40ХН2МА, 40Х2Н2МА, 36Х2Н2МФА, 30ХМА, 40ХФА;

– forced high-speed diesel engines – steels 18Х2Н4МА, 40ХН2МА, 38Х2Н2МА, 30ГМ;

– stationary and low-speed marine engines – steels 40Х, 45Х, 40ХН, 45Г2.

The properties of some alloys are shown in *Table 1*.

Table 1 – Properties of the steels and alloys used for the connecting rods

Parameter	Steel 40XH	Steel 40XH2MA (SAE-4349)	Steel 18X2H4MA	Titanium alloy Ti-6Fl-4V (США)	Aluminum alloy Д16	Composite material Д16+16%SiC
Density, ρ, g/sm^3	7.85	7.85	7.95	4.43	2.8	2.9
Hardness, HB	200 – 320	217 – 333	262 – 400	255 – 340	105	
Untimate strength σ_U, MPa	910	1000	940 – 1470	≥930	450	547
Yield strength, $\sigma_{0,2}$, MPa	710	850	710 – 1170	≥862	300	465
Compressive yield stress $\sigma_{-0,2}$, MPa	710	850	710 – 1170	917	285	-
Elasticity modulus, $E \cdot 10^{-3}$, MPa	204	204	150	105 – 115	71	110
Fatigue strength σ_{-1}, MPa	392 – 490	447	475 – 774	560	135	

The machining of the connecting rod must provide the accurate distance between the small end axis and the big end axis, and the distance between the pins of the link rods (the allowance is ±0.03 mm). It must also ensure the axes being mutually parallel. The faces of the web are polished and sometimes shot peened to improve the fatigue performances of the web. The ends of the connecting rod are bored out to press the bushes and the bearings inside. The bored out surfaces have the fifth or even fourth quality class and a very high-quality finish. In some instances, these surfaces are covered with chromium to avoid the scratches or any other damages, while pressing the bush in.

The centering shoulders of the rod (locking) bolts and the holes for their fitting are sometimes covered with chromium.

The acceptance of the connecting rods among the others includes the mass check out. As you know, the mass may vary within the range 15…20 grams from the connecting rod to the connecting rod.

The decision-making criteria for the material of the crankshaft bearings are all properties that characterize the durability (the sliding velocity, the temperature of the working layer, the specific pressure). The maximum acceptable sliding velocity for the modern antifriction alloys does not exceed 25 m/s. The limiting temperature of the working layer during operation is approximately equal to 120-130 °C (for the tin and lead babbitts), 140-150 °C (for the lead bronze and the tinny aluminum alloys). Data on the endurance of some sliding bearings are presented in *Table 2*.

Table 2 – Some properties of the sliding bearings

Material	Maximum working pressure, MPa	Pressure of the fatigue damage, MPa	Relative endurance
Tin babbitt (film width is 0.5 mm) on the steel base	5 – 7	12	1
Lead babbit (film width is 0.5 mm) on the steel base	5 – 8	15.5	1.3
Lead babbit (film width is 0.1 mm) on the steel base	8.5 – 15	19	1.6
30 % lead bronze (film width is 0.5 mm) on the steel base	-	35	2.9
30 % lead bronze (film width is 0.5 mm) on the steel base with a conformable lead alloy	15 – 20	53	4.4
Aluminum alloy, such as SAE 780	-	55	4.6
Aluminum alloy, such as SAE 780 with a conformable lead alloy	more than 20	57	4.7

The tin-based babbits have high antifriction and anti burning properties, high running-in ability, and corrosion resistance. But unfortunately, they soften very fast during operation.

The lead-based babbits have even higher bearing property and fatigue strength. Their short lifetime and high cost made the babbits to be excluded from being used for the sliding bearings of the modern aircraft and automotive piston engines.

The main bearings of the crankshafts of the forced piston engines are usually made of the binary alloys of the copper and the lead, called a lead copper. The spots of the soft lead, present on the surface of the copper-lead alloy, provide the latest with the outstanding antifriction properties. The antifriction properties grow with the lead percentage in the lead copper. Hence, the lead bronze with 25-40% lead is used for the sliding bearings.

Comparing to the other antifriction alloys, the lead bronze has high mechanical strength at high temperatures (80…180 °C). That is why it can successfully work at high pressure acting on the bearing. The major advantage of the lead bronze as material for the crankshaft is its ability to oppose the fatigue flaking. The fatigue life of the lead bronze bearings is several times longer than that made of lead or tin babbits. As the lead bronze does not soften a lot at high temperatures, so the temperature effect on the fatigue strength is negligibly small. If necessary, the fatigue strength of the lead bronze can be improved by the cold deforming.

At the same time, the lead bronze is harder to burn in with the crankpin journal. It absorbs the abrasive particles less, hence, it wears the crankshaft out more. The crankpin journals rotating in the lead bronze have high rigidity. The clearance between the crankpin journal and the bearing must be in-

creased. When the bearing interacts with the oxidized oil, the debris from the friction surfaces is dissolved. Less number of the lead spots causes the worse antifriction properties of the bearing surface. If the worst comes, the friction surface may become covered with scuffing.

To reduce the probability of the segregation, while covering the bearings with the bronze, the latest is mixed with small portions of silver, tin, nickel, manganese, sulfur (0.1%) in the form of sulfur galenite component.

The aluminum-based antifriction alloys have high fatigue strength, excellent heat conductivity, low specific weight and high rust-proof properties. To improve the antifriction properties, the alloys are admixed with soft metals, like cadmium, tin, lead. They generate the thin film on the bearing`s surface, which protects the bearing from being seized with the crankpin journal.

Comparing with the cast iron or the steel, the aluminum alloys have a high thermal expansion ratio. Hence, when the bearing is heated, then the thermal yield limit breaking stress may originate. The plastic deformations of the bearing may cause the crankshaft jamming or turning the bearing in the bed. So, to eliminate these harmful effects, the designers select the aluminum alloys with the increased yield strength and therefore with higher rigidity.

The aluminum alloys that were used for a single-bed sliding bearings have comparatively high rigidity. That is why they are of less hardness. They poorly absorb the debris available in the oil and have the insufficient run-in. Because of the high rigidity, the bearings made of aluminum alloys intensely wear out the crankpin journals. They are also characterized by an increased tendency to scuffing. Despite the increased strength of the aluminum alloys, the single-bed bearings made of them can be plastically deformed, and even jam the shaft. To prevent the deformations, the bearing width is increased (up to 5 mm). But this solution is too far away from the optimal. The usage of the bimetal bearings consisting of steel frame and a thin layer of aluminum antifriction alloy sounds to be a much better idea. Totally, the structural strength of the bimetallic bearings is determined by a strong steel base, so the working layer can be made of the softer aluminum alloy, having high run-in and absorption features. To improve the anti scuffing properties and the running-in of the aluminum alloys with the insufficient amount of the soft components, they are covered with (galvanic technique) the film of a lead- tin- cadmium alloy (15…20 μm). The high tin aluminum antifriction alloy developed by “Glassir plc.” became the most abundant for the bimetallic bearings of the piston engines.

5 QUESTIONS FOR SELF-CHECKING

1. What are the main purposes of the connecting rod in the ICE?
2. What are the main elements of the connecting rod?
3. What are the main differences between the centrally arranged and adjoin connecting rods?
4. Enumerate the specific features of the big end in different engine types.

5. What are the purposes of the big end bearing? Describe the construction and used materials.

6. How is the lower half of the detachable connecting rod fixed to the web?

7. Enumerate the requirements made to the bearing.

8. What are the specific features of the connecting rods of AM-42, VK-105, ASh-82, JUMO-205, DB-601?

6 REPORTING

1. Draw the generic schemes of the connecting rods.
2. Draw the end seal of the master connecting rod of the ASh-82 engine.
3. Describe the lubrication system of the connecting rod bearings.
4. Enumerate and give a brief characteristic of the materials used for the elements of the connecting rods.

7 STRENGTH ANALYSIS

7.1 Web analysis

When an engine operates, the web of the connecting rod experiences a variable in time force ***K***. The force compresses or tenses the web. In this conditions, the connecting rod might collapse (*Figure 13*).

Figure 13 – Connecting rod of the ROTAX-582 with the pin and the needle sleeve bearing

The most dangerous compression force that is considered in the strength analysis is a force of the gas pressure at the ignition moment

$$P_{g\,max} = \left(p_{g\,max} - p_{crankcase}\right)F_{pist}, \qquad (1)$$

where $p_{g\,max}$ is the maximum pressure of the working cycle;

$p_{crankcase}$ is pressure in the crankcase;

F_{pist} is a piston area.

The inertia of the reciprocating mass is neglected in this analysis. The inertia at the ignition moment reduces the force acting on the connecting rod.

The extreme magnitude of the tensile force corresponds to the TDC position of the piston at the end of the exhaust stroke. Neglecting the insignificant difference between the masses causing the inertia at different sections of the connecting rod, the inertia can be calculated as

$$P_{jn\ max} = -m_{res} \cdot R \cdot \omega^2 (1+\lambda), \qquad (2)$$

where m_{res} is the mass of the reciprocating parts;

R is a crank radius;

ω is an angular speed.

In this analysis, we will consider a compression stress as positive, and a tensile stress as negative.

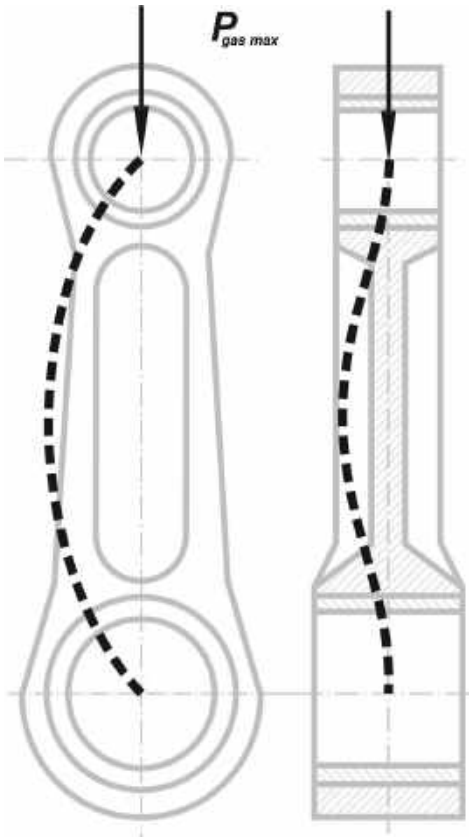

Figure 14 – Design scheme for the web analysis

If the web has the I-beam shape, then its strength must be individually determined in two mutually perpendicular planes: the hobbing plane and the perpendicular to it plane (see *Figure 13*).

The parameter of interest in this analysis is the fatigue strength. The design section depends on the web shape. If the web shape remains constant or almost constant along the web length, then the design section is in the middle of the web length $F_{I\text{-}I}$ (see *Figure 14*). Otherwise, the section of the smallest area is selected to be the design section (usually it is the section near the small end of the connecting rod $F_{II\text{-}II}$).

Let us consider the case when the middle section is acted by the compression force. Then we must consider not only the compression stress, but also the buckling. Finally, the total compression stress in the design section, when the connecting rod is buckled in the hobbing plane, can be evaluated as (see *Figure 14*):

$$\sigma_{max\ x-x} = P_{gas\ max}\left(\frac{1}{F_{I-I}} + 5{,}36 \cdot 10^{-5} \cdot \frac{L^2}{I_x}\right) \cdot 10^{-4}, \qquad (3)$$

where $F_{I\text{-}I}$, is an area of the design section, m^2;

I_x is the inertia of section $F_{I\text{-}I}$ about the axis x-x, m^4.

Following the designations in *Figure 15*,

$$I_x = \frac{B \cdot H^3 - (B - b)h^3}{12}. \quad (4)$$

The stress in the design section, when the connecting rod is buckled in the perpendicular to the hobbing plane, can be evaluated as

$$\sigma_{max\ y-y} = \max\left(\frac{1}{F_{I-I}} + 5{,}36 \cdot 10^{-5} \cdot \frac{L_1^2}{4 \cdot I_y}\right) \cdot 10^{-4}, \quad (5)$$

where I_y is the inertia of section F_{I-I} about the axis y-y, m^4,

$$I_y = \frac{(H - h)B^3 + h \cdot b^3}{12}. \quad (6)$$

If the design section of the web F_{II-II} is in the small end of the connecting rod, then only compression stress originates:

$$\sigma_{max} = \frac{P_{gas\ max}}{F_{II-II}}. \quad (7)$$

The highest negative stress in the design section (i. e. tensile stress) is

$$\sigma_{min} = \frac{P_{j\ max}}{F}, \quad (8)$$

where F is an area, that can be equal to F_{II-II} or F_{I-I} *(*it depends on which section is selected as a design one).

The average stress in the design section σ_m and the amplitude σ_a are

$$\sigma_m = \frac{\sigma_{max} + \sigma_{min}}{2} \quad \text{and} \quad \sigma_a = \frac{\sigma_{max} - \sigma_{min}}{2}. \quad (9)$$

In this case, the safety factor is determined as

$$n'_\sigma = \frac{\sigma_{-1}}{\sigma_a \cdot \frac{k_\sigma}{\varepsilon_\sigma} + a_\sigma \cdot \sigma_m}. \quad (10)$$

The coefficient a_σ depends on the material. For the steel 18XHBA

(σ_{-1} = 450…480 MPa) it can be set 0.12-0.16. The stress concentration coefficient k_σ depends on the shape of the cross-section. As the transition radiuses, the width of the web and the surface finish of different modern high-power engines are almost the same, then the stress concentration can be considered equal to a unity for the rough estimation of the fatigue strength. It is also acceptable to consider the dimension factor to be equal to unity $(\varepsilon_\sigma = 1)$. The acceptable safety factor for the webs of the connecting rods must be within the range 1.4-3.0 (see formula (10)).

The web of the master connecting rod of the star engine is loaded as with the forces acting itself, so with the variable in time forces from the link connecting rods. All these forces bend the web of the connecting rod. To oppose the bending moment, the inertia of the sections from the small to big end must be progressively increased.

7.2 Small end analysis

The section III-III in the small end of the connecting rod (see *Figure 15*) is tensed by the inertia of the piston assembly. The inertia gains the maximum value in the top dead center at the end of the exhaust stroke. When the connecting rod is loaded with the forces directed to the crank side, the section III-III also experiences this loading. Thus, the section III-III is loaded by the variable in time force. The force alternates from zero P = 0 to max value P = P_{max}.

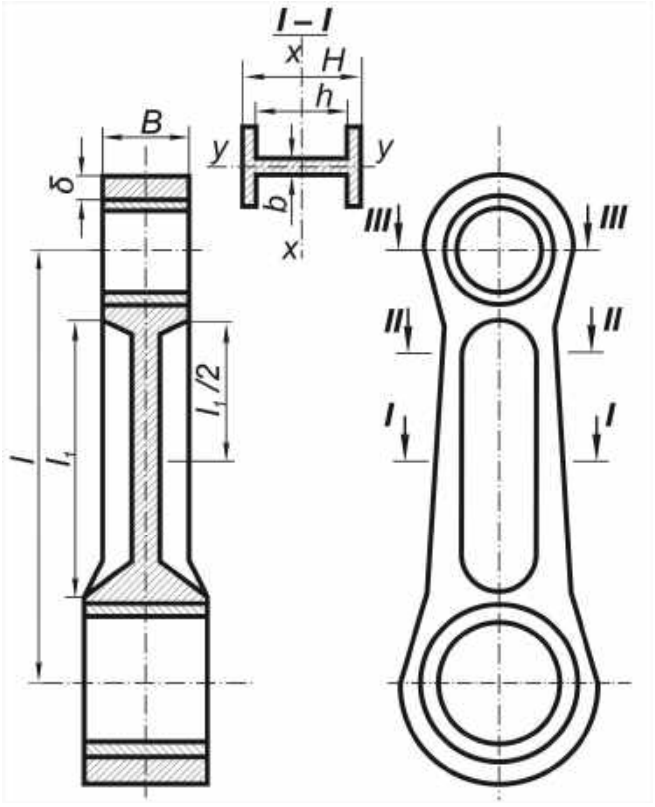

Figureure 15 – The design scheme of the connecting rod

The alternation obeys the so-called pulse loading cycle:

$$P_{max} = P_{j\,pist\,max} = -m_{pist} \cdot R \cdot \omega^2 (1+\lambda). \qquad (11)$$

The maximal tensile stress in the design section are

$$\sigma_{max} = \frac{P_{max}}{2 \cdot \delta \cdot a}. \qquad (12)$$

The additional stress in section III – III, caused by pressing the bush in the small end, are usually neglected. According to the pulse loading cycle, the average stress σ_m is equal to the amplitude σ_a:

$$\sigma_m = \sigma_a = \frac{\sigma_{max}}{2}. \quad (13)$$

The safety factor is determined as

$$n'_\sigma = \frac{\sigma_{-1}}{\sigma_a \frac{k_\sigma}{\varepsilon_\sigma} + a_\sigma \cdot \sigma_m} = \frac{\sigma_{-1}}{\frac{\sigma_{max}}{2}\left(\frac{k_\sigma}{\varepsilon_\sigma} + a_\sigma\right)}. \quad (14)$$

The variables σ_{-1} and a_σ are the same as in the formula (10). The stress concentration k_σ depends on the number of the drillings in the design section and the finishing of the surfaces. The stress concentration must be within the range 1-2. The coefficient ε_σ can be set equal to unity. The safety factor, which has been determined in the equation (14) must not be less than 4. The pressed bronze bush is checked for the specific load by the formula

$$k_{bush} = \frac{p_{gas\,max}}{D_{bush} \cdot a}, \quad (15)$$

where a is a length of the bush, m;

D_{bush} is the diameter of the bush, m.

The value of the k_{bush} for the bronze bushes must be within the range 40…70 MPa.

7.3 Big end analysis

The big end of the master connecting rod has a very complex shape. It experiences the forces arriving from the pistons of the master and link connecting rods. It is impossible to carry out more or less precise analysis of the big end of the master connecting rod. The big end of the link rod can be analyzed similar to the small end manner using the formula (14). But in this case, the inertia force must include not only the inertia of the piston mass, but also the inertia of the link rod itself. The analysis of the link rod pin is a bit different from the analysis of the piston pin. In the case of the link rod pin, the loading cycle is asymmetrical (because the pin is pressed in the connecting rod). The maximum

force, which causes the pin bend, is directed to the crank side. It can be calculated as

$$P_{max\,1} = P_{gas\,max} - P_{j\,max}. \tag{16}$$

The maximum force acting to the opposite side can be calculated as

$$P_{max\,2} = P_{j\,max} \approx -m_{pist} \cdot R \cdot \omega^2 (1+\lambda), \tag{17}$$

where m_{pist} is the mass of the link connecting rod – piston assembly (the mass of the link rod is conditionally assigned to the reciprocating part mass).

The bending moment (M_{bend}) acting on the pin of the link connecting rod is determined as

$$M_{bend} = \frac{P_c}{2}\left(\frac{L}{2} - \frac{a}{4}\right). \tag{18}$$

The ultimate positive and negative stress are the following:

$$\begin{aligned} \sigma_{max} &= \frac{P_{max\,1}}{2W_{bend}}\left(\frac{L}{2} - \frac{a}{4}\right); \\ \sigma_{min} &= \frac{P_{max\,2}}{2W_{bend}}\left(\frac{L}{2} - \frac{a}{4}\right). \end{aligned} \tag{19}$$

The safety factor can be evaluated according to the formula (10) and known average stress σ_m and amplitude σ_a. The maximum specific pressure acting on the bronze bearings of the big end of the link connecting rod might be increased to 95 MPa thanks to the better lubrication of the small end. The specific pressure of the pin on the holes in the master connecting rod can be set 100-120 MPa because the pin is fixed.

7.4 Analysis of the rod bolt

The rod bolts are loaded with the force $P_{j\,rod\,bolt}$, which tears the connecting rod from its big end lower half. The force includes the inertia of the piston and the connecting rod in the TDC:

$$P_{j\,rod\,bolt} = P_{j\,pist} + P_{j\,conn\,rod\,rot} = -\left[m_{pist}(1+\lambda) + m_{conn\,rod\,rot}\right] R \cdot \omega^2, \tag{20}$$

where $m_{conn\,rod\,rot}$ is the mass of the connecting rod part that was assigned to the rotating mass (without the mass of the lower half of the connecting rod).

The force $P_{j\,rod\,bolt}$ additionally loads the rod bolts, which were tensed by the pull force P_{pull}. However, it unloads the joint between the connecting rod and its lower half of the big end. In a real practice the 20-25 % of the force $P_{j\,rod\,bolt}$ loads the rod bolt, and 75-80 % – unload the joint. The pull force is selected in the way to make the force $P_{j\,rod\,bolt}$ being 3 – 4 times greater than the unloading force.

Thus the pull fore can be calculated as

$$P_{pull} = (3...4)(0.75...0.80)P_{j\,rod\,bolt} \approx (2.5...3.0)\cdot P_{j\,rod\,bolt}. \quad (21)$$

The maximum tensile force:

$$P_{bolt\,tens} \approx P_{pull} + 0{,}25\cdot P_{j\,rod\,bolt}. \quad (22)$$

As the variable portion of the total force is very small, its strength can be estimated using the maximum static stress as

$$\sigma_{rod\,bolt} = \frac{P_{rod\,bolt\,tens}}{i\frac{\pi}{4}\cdot d_{int}^2}, \quad (23)$$

where ***i*** is a number of bolts;

d_{int} is the internal diameter of the thread.

It must be noticed that usually the most dangerous section of the rod bolt is some section with the thread, even if the bolt body is of lower diameter than d_{int}.

8 QUESTIONS FOR SELF-CHECKING

1. Describe the forces acting on the components of the connecting rod and the strains they generate.
2. Describe the web analysis.
3. Describe the analysis of the small end.
4. Describe the analysis of the big end.
5. What are the specific features of rod bolt analysis?

9 REQUIREMENTS

The following requirements must be met when conFigureuring the crankshaft:

– the crankshaft must have length enough to place the definite number of connecting rods considering the cylinder conFigureuration;

– uniform alternation of power strokes among the cylinders;

– dynamic balance;

– strength requirements;

– the dangerous resonant torsional oscillations must be outside the crankshaft operational range;

– low mass;

– manufacturability.

10 GENERAL ARRANGEMENT

Crankshaft consists of the following main elements (*Figure 16*):

– main journals serving for securing the crankshaft in the bearings mounted in the crankcase (also known as main bearings);

– crankpin journals that connect the big ends of a connecting rod with the crankshaft;

– webs, coupling the main journals with the crankpin journals;

– flywheel mounting flange for power takeoff (taken power is spent to drive the propeller – aircraft use, or accessory gearbox – car use);

– crank nose usually used to drive different accessories, pumps, supercharger etc., which are mounted on the crankcase.

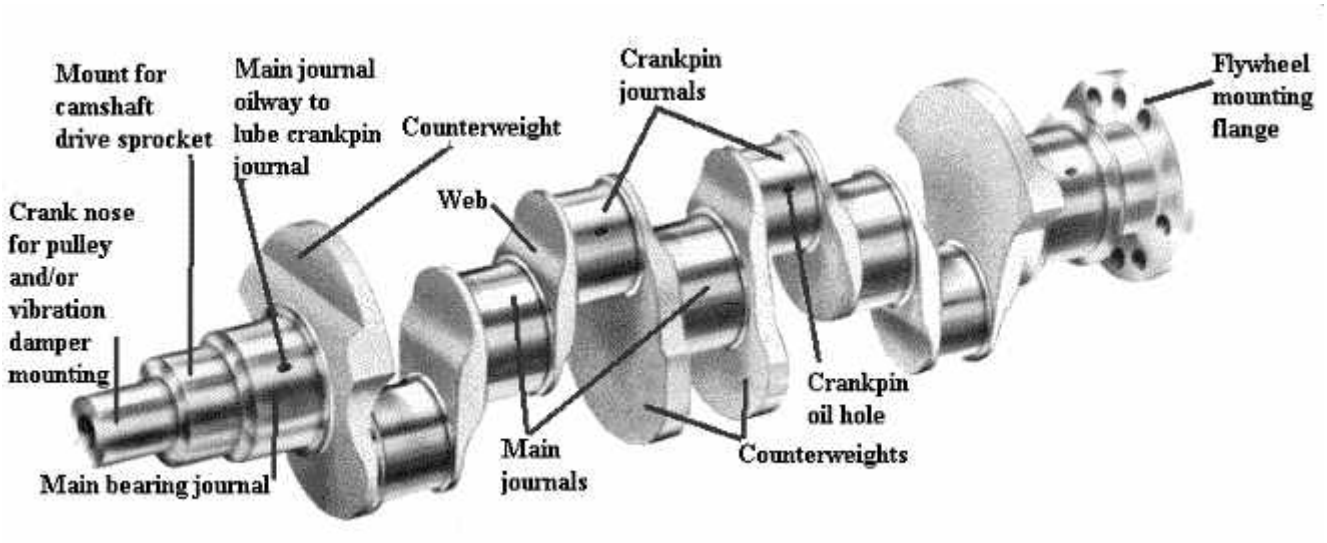

Figure 16 –Generic scheme of an in-line engine

The assembly of the crankpin journal, two webs and the adjoining main

journals is termed crank.

11 DESIGN PROPORTIONS FOR THE CRANKSHAFTS

The crankshaft proportions of the in-line engine are considerably different from the star engine ones.

The crankshaft of the in-line engine is manufactured one-piece with the detachable main and crankpin sliding bearings. The main sliding bearings are detachable to make the assembling possible.

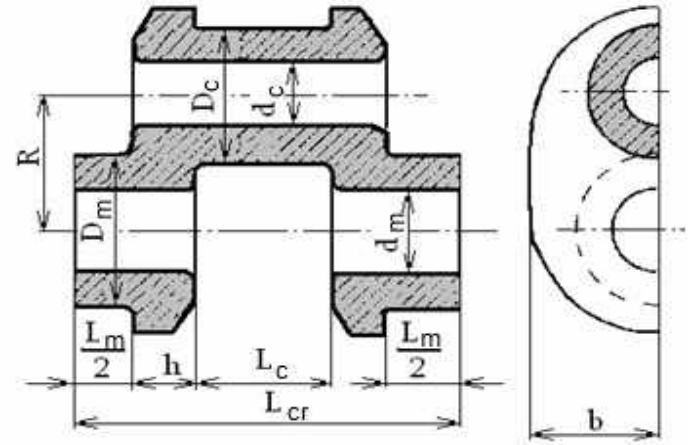

Figure 17 – Generic scheme of a crank

The crankshaft of the star engine is usually designed split. The spit crankshaft gives some profits. For example, the heavily loaded big end of the master connecting rod can be designed without the splits and the ball bearings can be used in the main supports. The ball bearing has small axial size, which lets designers implement the small main journals. In this case, the thicker webs and the longer crankpin journals can be used, which is extremely important for engines with numerous cylinders linked to the single crank. The majority of the crankpin journals rest on the sliding bearings to make the mass distributed to the crankpin journal minimal and to make the crankcase overall sizes low. Main sizes of the crankshaft are presented in *Figure 17*. The relations of these sizes are shown in *Table 3*.

Table 3 – The relations of crank sizes

Crankpin journal			Main journal			Web			Others	
$\frac{D_c}{D^{*)}}$	$\frac{L_c}{D_c}$	$\frac{d_c}{D_c}$	$\frac{D_m}{D}$	$\frac{L_m}{D_m}$	$\frac{d_m}{D_m}$	$\frac{h}{D}$	$\frac{b}{D}$	$\frac{S}{D}$	$\frac{S}{D_c + D_m}$	$\frac{L_{cr}}{D}$
In-line engine										
0.5	0.8	0.63	0.593	0.5	0.67	0.135	0.79	1.04	1.15	1.12
0.57	0.96	0.67	0.665	0.635	0.72	0.175	0.96	1.185	0.86	1.15
Star engine										
0.5	0.965	0.43	0.58	0.35	0.43	0.22	0.58	1.00	1.00	1.25
0.6	1.10	0.74	0.78	0.34	0.612	0.48	0.90	1.23	0.72	1.47

*)D is a cylinder diameter, S is a piston stroke.

Designers of the aircraft piston engines relentlessly strive to

- make the crankshaft stronger;

– improve the bending and torsional rigidity;

– use the physical properties of the crankshaft to the full extent, i.e. make it lighter by all means.

12 ARRANGEMENT AND SHAPE OF THE CRANKS

Aircraft in-line engine can be equipped with the single-, two-, four- and six-crank crankshaft. The automotive engine may also have five crank crankshaft (*Figure 18*).

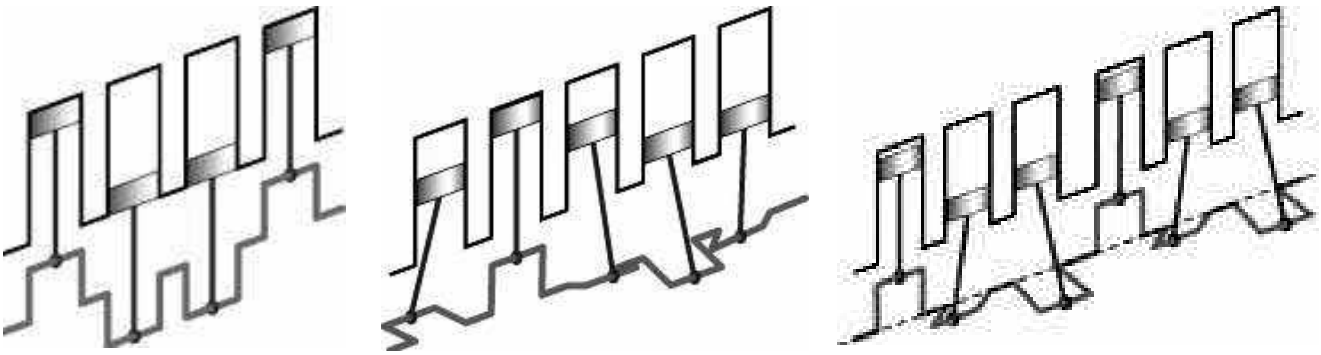

a b c

Figure 18 – The generic schemes of in-line engines:
a – four-crank; b – five-crank; c – six-crank

The cranks of the four-crank crankshaft are usually arranged in a common plane. The cranks of the six-crank crankshaft are mutually angularly spread at 120 degrees. The considered crankshafts are symmetrical to the center of their middle main journal, i.e. both parts of the crankshafts are similar relative to the center of their middle main journal. Such crankshafts are the most balanced providing the correct ignition sequence in the cylinders. The cranks of the five crank crankshaft are mutually angularly spread at 72 degrees. An optimal operational sequence of the four stroke five-cylinder engine is 1-2-4-5-3, which are cylinder numbers. The machinery of each cylinder contains two counterweights attached to the shaft. The specially arranged misbalance of the flywheel and the damper on the frontal crankshaft`s end absorb the torsional oscillations. The in-line five-cylinder engine is designated as I5 or L5 «Straight–5», «In–Line–Five» as it is shown in *Figure 19*. The L5 conFigureuration is unbalanced.

The in-line five-cylinder engines are very rear to be used in automotive vehicles. Nevertheless, exceptions happen. The first company to present the five-cylinder automotive engine was Audi AG for Audi 100. The engine was positioned as that one who had absorbed the advantages of four and six cylinder engines. Engines of the mentioned conFigureuration were used by the Audi, Volvo, Ford, Mercedes–Benz, Honda, Land Rover, Fiat, Lancia and some others.

Engine with the smallest displacement volume was Audi 100. The volume

was 1921 cubic centimeters.

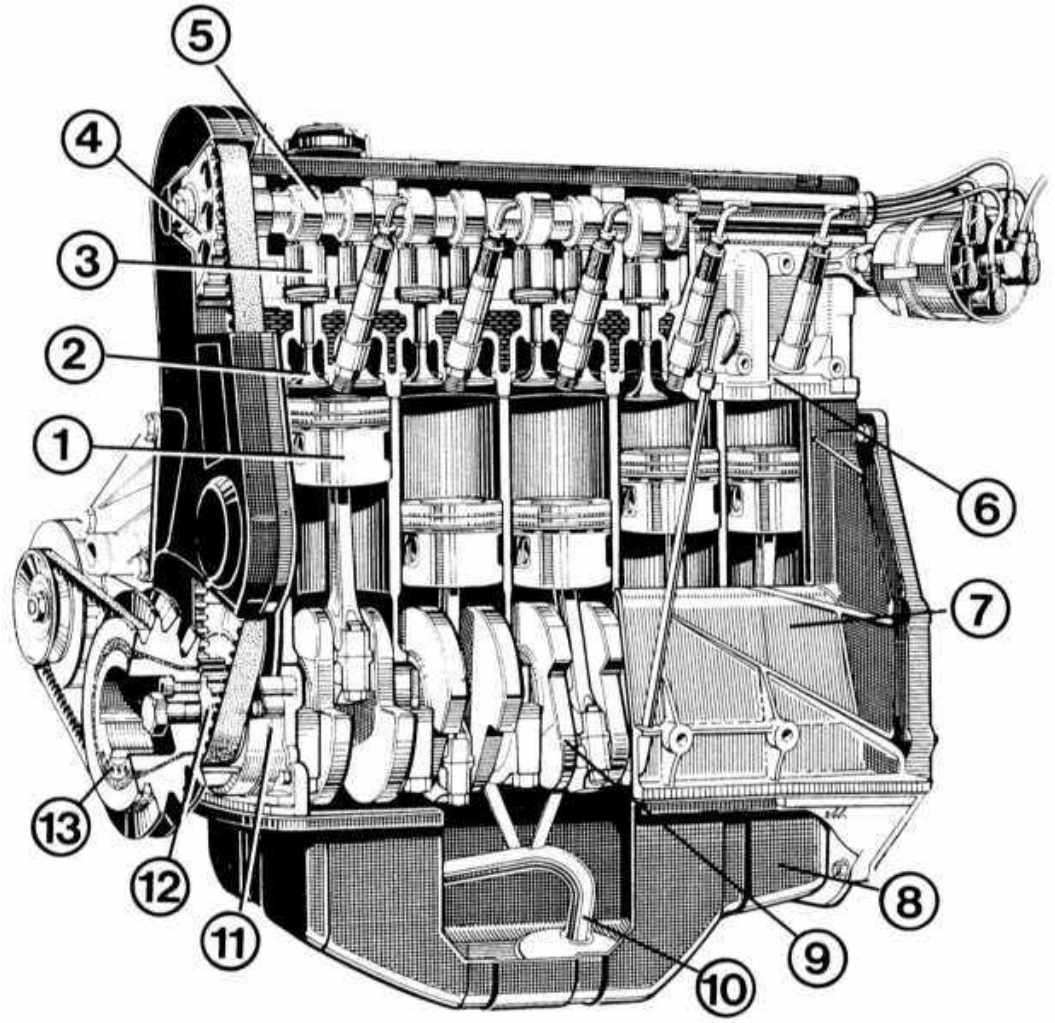

Figure 19 – Five-cylinder engine NG (98 kW):
1 – piston; 2 – valve; 3 – hydraulic tappet; 4 – timing pulley of a cam shaft;
5 – cam shaft; 6 – cylinder head; 7 – cylinder block; 8 – oil pan;
9 – crankshaft; 10 – intake pipe of the oil pump; 11 – oil pump;
12 – timing pulley of the crankshaft;
13 – V-belt pulley with vibration damper on the crankshaft

The big two stroke five-cylinder in-line engines found wide use in shipbuilding.

In order to prevent the crankshaft sagging in maintenance, the four-cylinder engine is equipped with five supports and five-cylinder engine – with six supports (main journals). Each crank is designed to be supported by the bearing on a left and right sides. The six-cylinder engine has another construction. Due to economy considerations, two connecting rods are placed between the main bearings. So, such engine has totally 4 main bearings. So let us consider the six-cylinder AM-38 crankshaft presented in *Figure 20* as an example. The oil cavities in the Figureure are shaded gray.

The crankshafts of the star engines have single or two cranks (single- or two-row star respectively), see *Figure 21*.

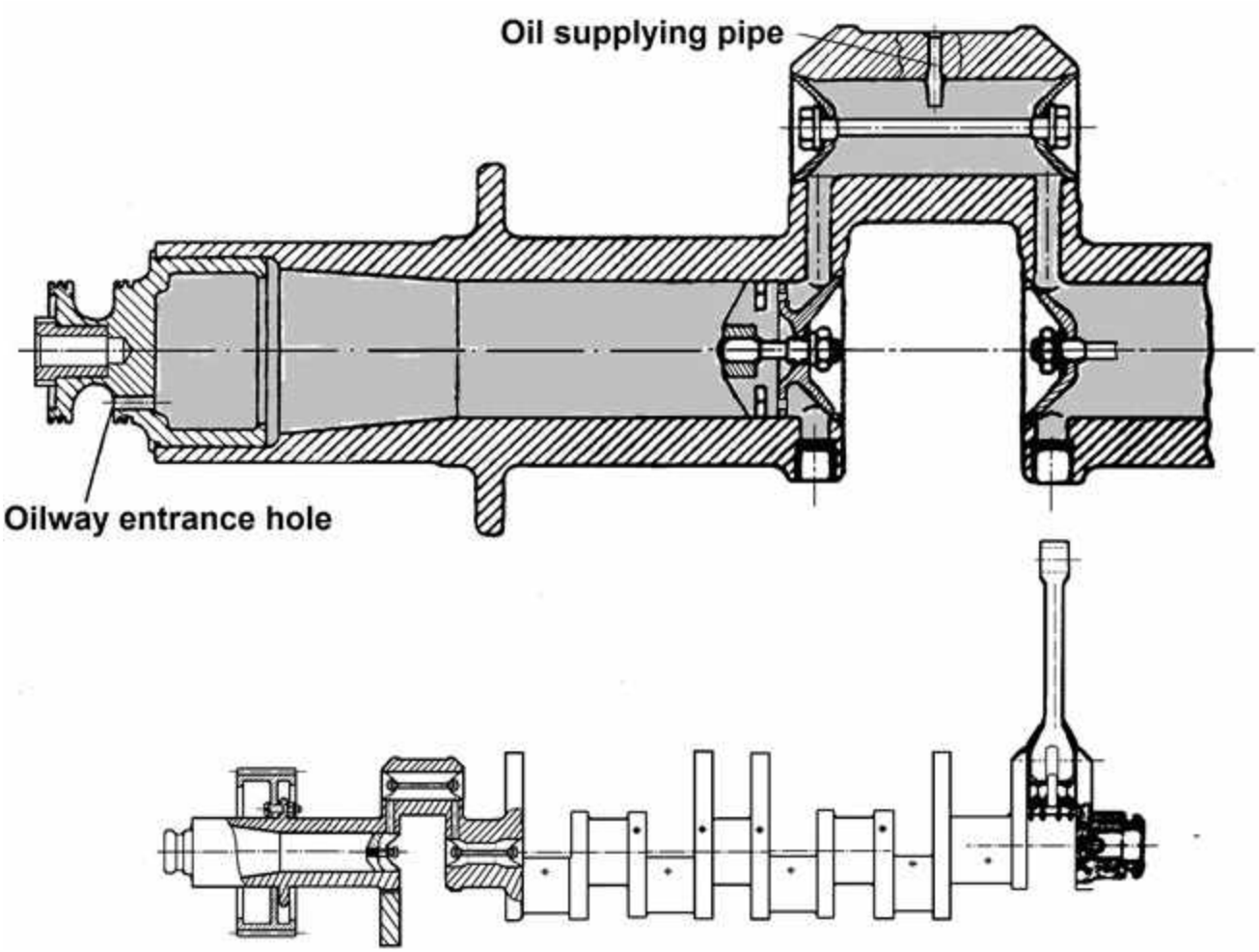

Figure 20 – Crankshaft scheme of AM-38 engine

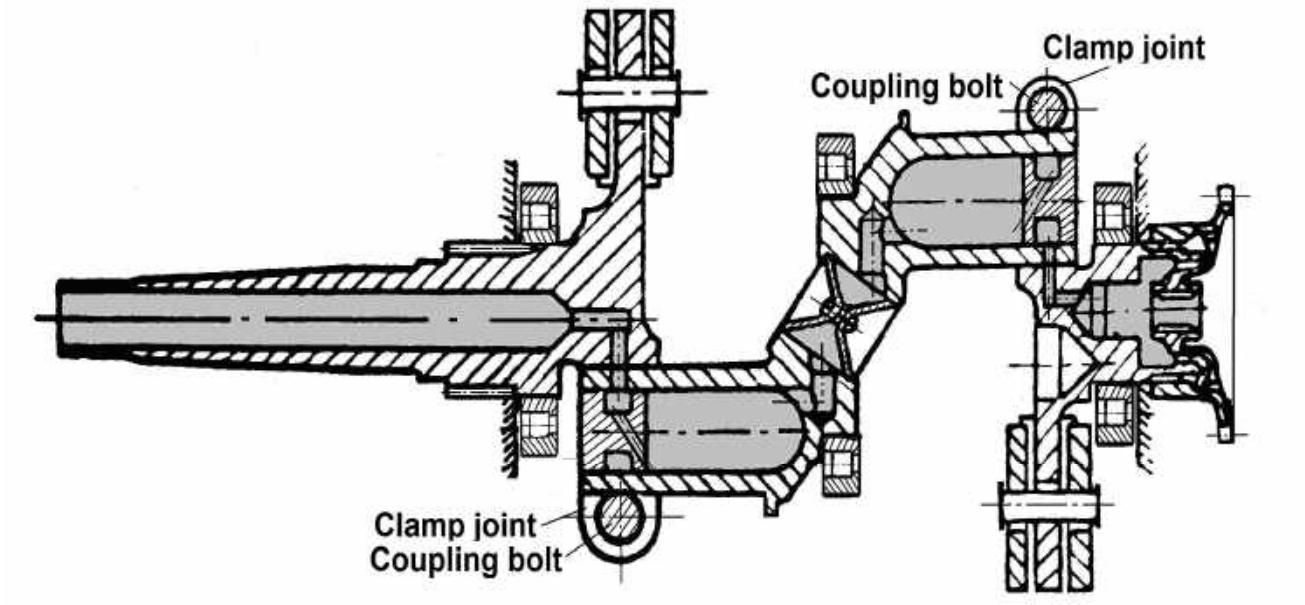

Figure 21 – The scheme of a two-row star engine crankshaft

13 CRANKSHAFT COMPONENTS

The sizes of the crank components (journal diameters, web sizes etc.) must be selected to meet the strength requirements and load the bearings with the acceptable specific loads. The design must also be rigid enough to have the minimum straining during operation. This gives benefits for the bearing operational conditions.

Holes are drilled in the journals and then bored.

The holes in the main and crankpin journals are usually blanked off from the ends.

The formed cavities serve for oil supply to lubricate the friction pairs. The cavities in the separate journals are interconnected by the holes in the journals and the webs forming the common oil reservoir for the entire crankshaft (or some cranks).

The debris is deposited at the periphery of the crankpin hole. To avoid the dust from getting in the crankpin bearing, the oil is supplied to the friction surfaces through the special pipes, which take it from the middle part of the cavity. The pipes expand in the rod journal to constrain the displacements (see *Figure 20*).

The oil holes must not be drilled in the loaded parts of the friction journals because this may drastically decrease the bearing capacity.

14 CRANKSHAFT BEARINGS

The sliding bearings are usually used in the main and crankpin journals of the in-line engine and in the crankpin journals of the star engine. The main and crankpin bearings experience high specific load (up to 22 MN/m^2) and operate at high circumferential velocities (10-15 m/s). Because of the hazard operational conditions, the bearings frequently limit the engine operation time and may cause the earnest accident. The powerful tool to improve the carrying capacity is the forced oil supply at 0.3-1 MPa pressure.

The in-line engine has the oil supply through the external pipeline to each main journal individually, e.g. VK-105. From the main journal, oil gets to the main journal cavity and next – to the oil clearance of the connecting rod bearings. The lubrication system like this is called an individual. In some instances (engines AM-38, AM-42, see *Figure 20*) oil is supplied from the ends of the crankshaft through the dummy bearings and passes through the entire crankshaft, progressively lubricating all main and crankpin journals. The dummy bearings are sealed by the C-rings. The main advantage of this system, known as a central lubrication system, is a good oil filtering while it passes through the webs. Here the mechanical impurities are centrifuged. The disadvantages of the central lubrication system are the necessity to have the great holes in the webs to pump the great oil flow and considerable oil heating that leads to the oil viscosity drop. These disadvantages are partially compensated if the oil is supplied from the both sides.

The historical progress of the main bearings is shown in *Figure 22*. The sliding bearing consists of the bronze or steel base and the babbitt or lead bronze priming.

Nowadays the thin-wall bearings (see *Figure 22*, e) made of thin steel strip are the most abundant. The steel base is 1.6-2 mm width and the priming is 0.5 – 0.7 mm.

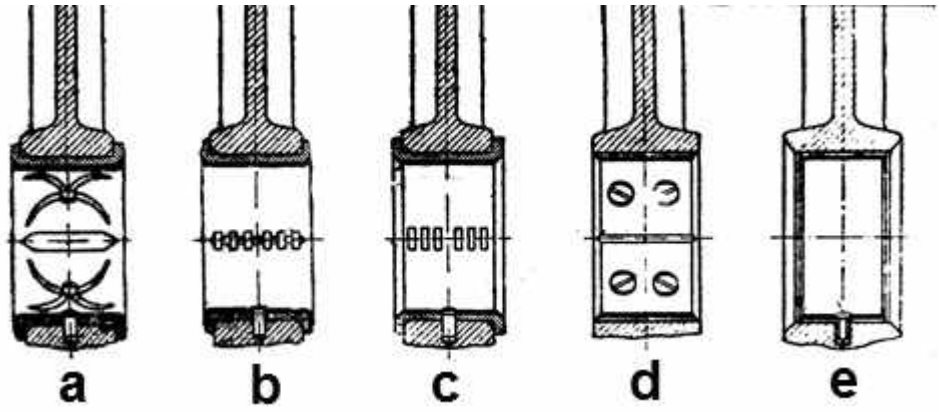

Figure 22 – Historical progress of the main bearings

15 WEBS

The webs are the most loaded crankshaft parts. In the piston engine infancy, the webs had been prismatic (*Figure 23*, variants 1 – 3). Nowadays, to increase the working surface of the crankshaft journals designers reduce the web thickness and increase their width. First, designers kept the prismatic web shape and increase the central part, or made the web rhombic (variants 4, 5). Finally, they switched to the elliptical webs (variant 6). Such a design is implemented for the AM-38 engine. The next progress step was the round webs (variant 7) used in some European, Korean, Japanese and American cars. Nowadays, the non-operable web parts are eliminated to make the construction lighter.

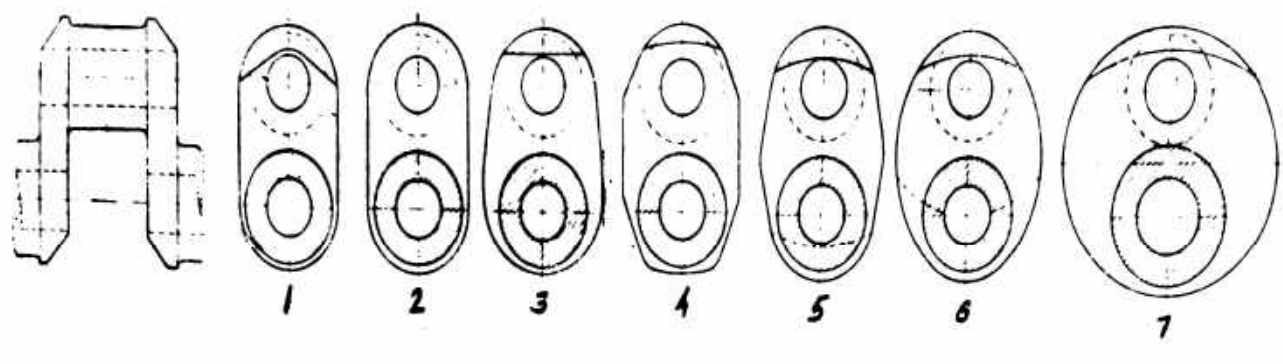

Figure 23 – Web designs

16 COUNTERWEIGHTS

The crankshaft of modern aircraft engines usually has the counterweights, which functions are:

- inertia forces and moments balancing;
- unloading main bearings from the centrifugal force;
- removing the resonant torsional oscillations outside the operational range;

The V-shape engines have six, eight or even twelve webs with the counterweights (webs of the middle main journal must obligatory be counterweighted). The counterweights also reduce the deformations caused by the inertia and improve the operational conditions of the main and crankpin journals.

For the counterweights` mass reduction it is expedient to make them as distant as possible from the crankshaft axis. The maximum radius is limited by the ability of the counterweight to pass in the crankcase, near the bottom of a cylinder liner and piston skirt. Pistons approach the counterweight the most in the BDC.

Usually, the counterweights are bolted or pinned to the web extensions.

The counterweights also serve for torsional oscillation damping in the modern star aircraft engines.

An aircraft propeller rotates at constant velocity ω_{prop} thanks to the high inertia (see *Figure 24*). That means that the reactive moment of the propeller will be constant too. The crank also experiences the variable by value and direction circumferential force T, which generates the variable in time torque. This torque is among the sources of the crankshaft rotation. The misbalance between the reactive moment and the torque causes the shaft twisting to different sides. As the result, the crankshaft will rotate at a variable in time angular velocity ω_{cr}.

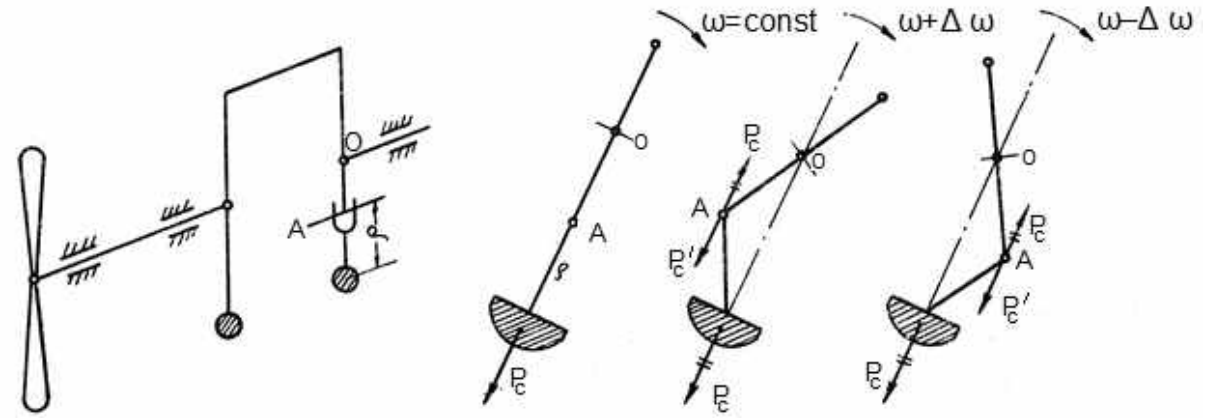

Figure 24 – The pendulum damper scheme: a – constant rotational speed; b – acceleration; c – deceleration

Thus, it originates two oscillation types:

- oscillations caused by the non-uniform torque (forced oscillations);

– oscillations initiated by the elastic forces (natural oscillations).

As torque value periodically repeats itself so at some mode engine may go to the resonance (the condition when the natural frequency becomes equal to the frequency of the forced oscillations).

To suppress the torsional oscillations the designers introduce the so-called oscillation dampers. Pendulum damper became the most abundant for star engines.

The generic scheme of the pendulum damper is presented in *Figure 24*. The pendulum with arm AB and mass G is studded to the web extension. When the rotational speed is constant the pendulum axis AB becomes collinear with a crank web axis OA (see *Figure 24, a*). The pendulum mass generates the centrifugal force P_c.

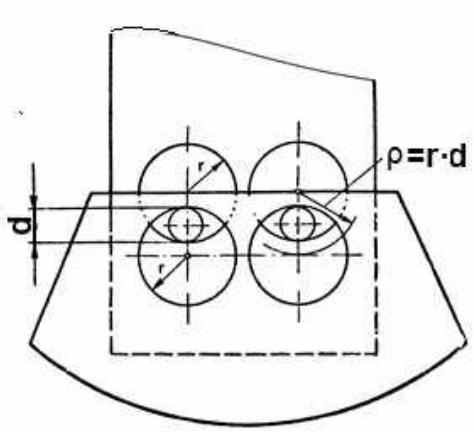

Figure 25 – Bifilar suspension scheme of the pendulum damper

The web outstrips the propeller at one moment (see *Figure 24, b*) and lags at the next one (see *Figure 24, c*) when the crankshaft oscillates. The pendulum with great inertia is willing to further motion at constant angular speed. Hence the pendulum will deflect from the web axis (see *Figure 24, b, c*). Let us shift the P_c to the point A. For this, we apply two forces at the point A, which are equal to P_c by value but opposite by direction. When considering the three force system we can separate out the forces couple (it is designated with a double dash) and P'_c force that will attempt to stand the shaft twisting relative to the crankshaft axis.

It is obvious that the pendulum will oppose the shaft twisting at any moment of time only in the case if its oscillation period is equal to crank oscillation period (by other words – equal to the disturbing force period). The fulfillment of this condition determines the pendulum swing radius ρ.

Usually, the analytical pendulum length ρ is relatively low (5 – 7 mm). Hence the heavy pendulum hang on the problem is solved by double pinning the counterweight. The diameter of the pins is less than the diameter of the holes in the web and the counterweight by the magnitude is equal to the pendulum length ρ (*Figure 25*). At the same time the pendulum mass is selected to fulfill the balancing condition.

17 JOINTS OF DETACHABLE CRANKSHAFTS

The detachable crankshaft of the star engine is typically clipped using the cut lug of the webs (*Figure 26, b*). They are next bolted together.

In this case (M-11, ASh-62, AI-26, AI-14 engines) the free end of the crankpin journal is brought in the cut lug of the rear crankshaft web (*Figure 26,*

a). Next, the lug is pulled. The pull force must be high enough for tight contact along the entire cylindrical surface of the groove on the web and for torque transfer.

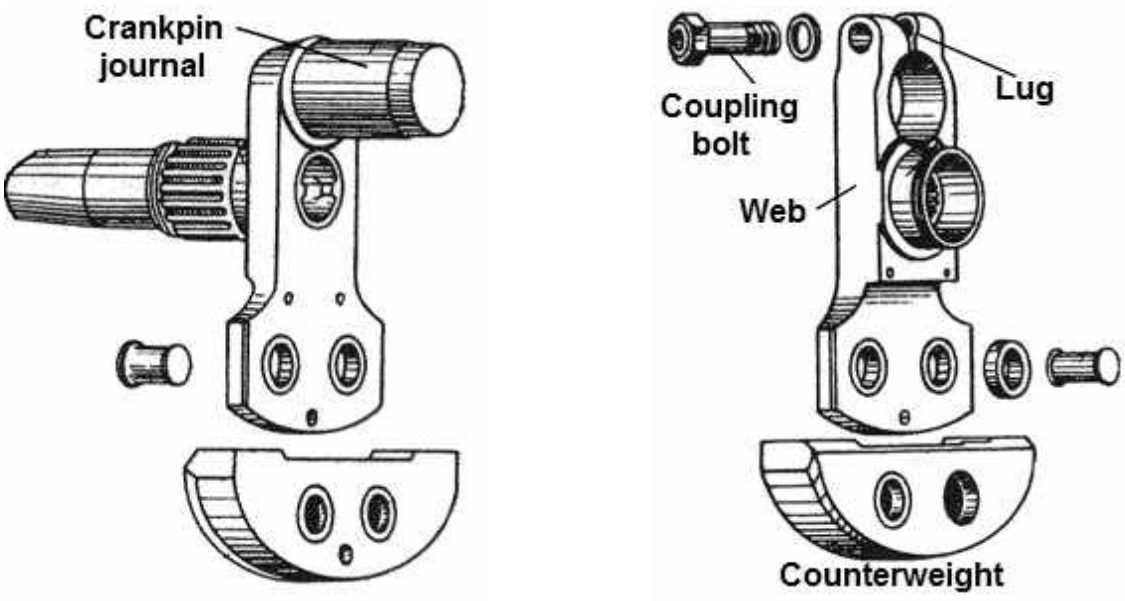

Figure 26 – The components of a detachable crankshaft of a star engine:
a –clipped using the cut lug of the rear crankshaft web;
b – clipped using the cut lug of the webs

The crankpin journal of the star engines with screwed crankshafts is manufactured bodily with the front web to avoid torque transfer from propeller drive through the cut.

The rear counterweight in this design is heavier than the front one because it balances the added mass of the coupling bolt and the lug.

The clipped joint of the shaft parts is simple by design and is simple to produce. One more advantage is the fact that the most heavily loaded crankpin journal parts are not weakened. The relative disadvantages of this construction are its relatively big overall sizes and mass of the rotating crank parts and different counterweights by design.

18 AXIAL FIXATION

Crankshaft must be strongly fixed axially in the crankcase. Such axial fixation is required to mutual position of the crankcase, crankshaft and parts attached to them and transfers axial loads from the shaft to the crankcase. These loads appear as the result of machinery operation (engine thrust of the gearless piston engine, the presence of bevel and helical gearings and so on) and because of arbitrary production errors during machining and assembling.

The crankcase and the crankshaft are made of different materials like alu-

minum and steel, which have different linear expansion factor. That is why the axial fixation is arranged in one place.

The crankshaft of the star engine with the ball and roller bearings on the main journals are fixed by one of these bearings.

So, axial fixation of the ASh-62IR crankshaft is made by the roller bearings of the front main journal. It is fixed in the wall of the middle crankcase (see *Figure 27*).

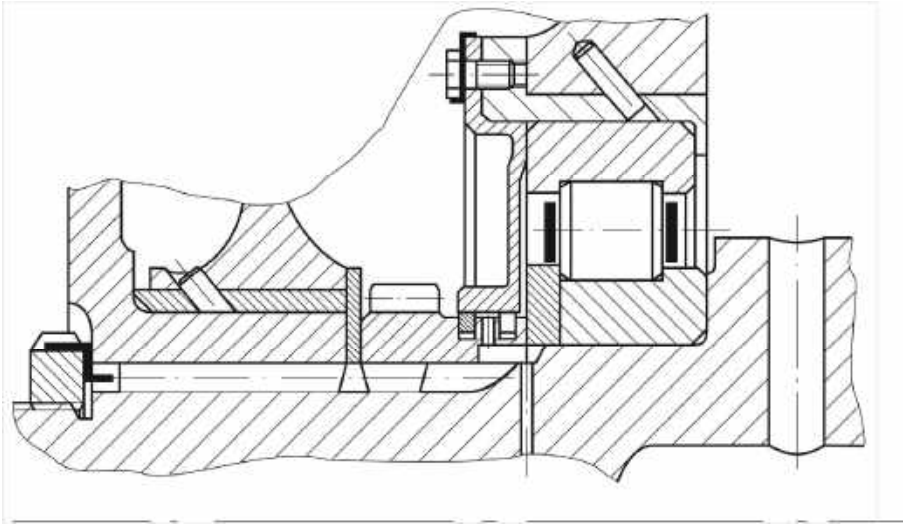

Figure 27 – The axial fixation of the ASh-62 cranshaft

19 BALANCING

The inertia of reciprocating and rotating crankrod parts belong to the main external forces of the engine. Balancing of these forces is the task of engine balancing.

The balancing can be arranged in two ways:

– self-balancing, which is possible only in the multi-cylinder engines (it is achieved only by the special cylinder arrangement which is not always acceptable);

– balancing with the counterweights.

The full-balanced engine means the engine with the inertia of rotating mass $P_{j\ rot}$ and inertia of reciprocating mass (primary $P_{j\ res\ 1}$ and secondary $P_{j\ res\ 2}$ misbalance) and their moments balanced.

19.1 Single cylinder balancing

The habitual single cylinder engine cannot be self-balanced. So let us discuss the scheme of its balancing by means of the counterweights.

The misbalance of the rotating mass is eliminated by the counterweights in the web extensions.

The $P_{ij\ 1}$ is directed along the cylinder axis. It cannot be balanced by the

above-mentioned counterweights.

To generate the similar force with the opposite direction designers add two counterweights which rotate at the same rotational speed to opposite directions. The initial counterweights` position is the most bottom ($\alpha = 0$). These counterweights are driven by the crankshaft and rotate at the speed ω. They produce only vertical component of the inertia by the centrifugal forces. The balancing force always meets the following condition:

$$2 \cdot P_{c1} \cdot \cos\alpha = -P_{j\,res\,1}. \tag{24}$$

Let us solve the right part of the equation

$$2 \cdot m_1 \cdot R_{res1} \cdot \omega^2 = -m_{res} \cdot R \cdot \omega^2, \tag{25}$$

where m_1 is a counterweight mass, R_{res1} is a radius of a counterweight gravity center, m_{res} is a mass of the reciprocating parts, R is a crank radius and find mass m_1

$$m_1 = \frac{-m_{res} \cdot R}{2 \cdot R_{res\,1}}. \tag{26}$$

The force $P_{j\,res\,2}$ same to force $P_{j\,res\,1}$ always matches the cylinder axis but it varies twice faster. That is why the $P_{j\,res\,2}$ balancing requires one more pair of counterweights.

They also rotate to the opposite sides but at a doubled rotational speed. This gives the resultant force, which varies twice faster $(2 \cdot \omega)$. The balancing condition looks like the following:

$$2 \cdot P_{centr\,2} \cdot \cos 2\alpha = -P_{j\,res\,2}. \tag{27}$$

Let us enter the left part and the right part

$$2 \cdot m_1 \cdot R_{res\,2} \cdot \omega^2 = -m_{res} \cdot R \cdot \omega^2, \tag{28}$$

where m_2 is a mass of a secondary counterweight;

$R_{res\,2}$ is the radius of a gravity center of the secondary counterweight, and find m_2

$$m_2 = \frac{m_{res} \cdot R \cdot \lambda}{8 \cdot R_{res\,2}} \qquad (29)$$

Finally, we have obtained a complex system known as Lanchester mechanism (see *Figure 28*). It provides the complete single cylinder balancing.

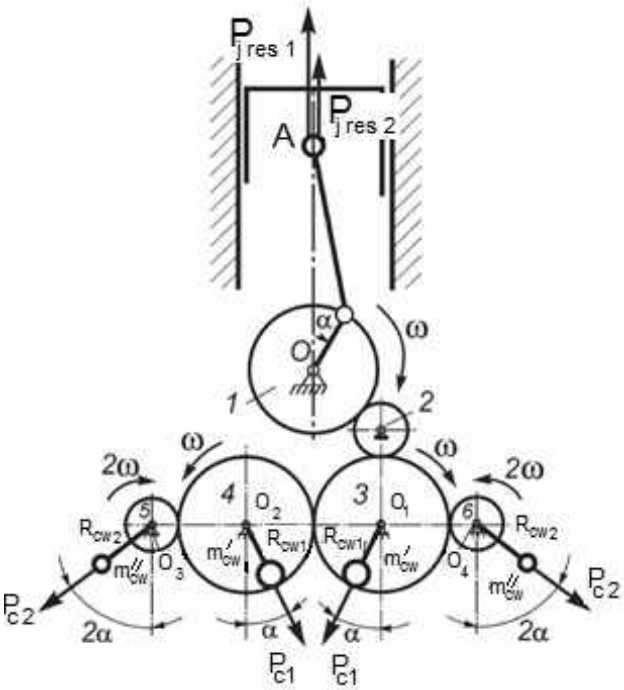

Figure 28 – The Lanchester scheme

19.2 In-line engine balancing

The multi-cylinder engines can be designed self-balanced in the case of definite cylinder arrangement.

The mutual balancing of inertia forces generated by the rotating parts is achieved by the crankshaft shape. It is important to make the crankshaft balanced by the forces and the moments of these forces.

Figure 29 contains the crankshaft schemes with balanced forces and moments (a) and with balanced forces but unbalanced moments (b).

Let us consider the reciprocating mass balancing.

Pay attention that forces $P_{j\,res\,1}$ and $P_{j\,res\,2}$ are two times different by the frequency. Hence they cannot balance each other.

The force $P_{j\,res\,1}$ can be expressed as a projection of some rotating vector $\vec{C}_1$. The vector rotates at the equal to crankshaft speed ω around crankshaft axis in the plane perpendicular to the latest plane. The absolute value of the vector is equal to the maximum force $P_{j\,res\,1\,max}$, which occurs at $\alpha = 0$:

$$\left|\vec{C}_1\right| = M_n \cdot R \cdot \omega^2. \qquad (30)$$

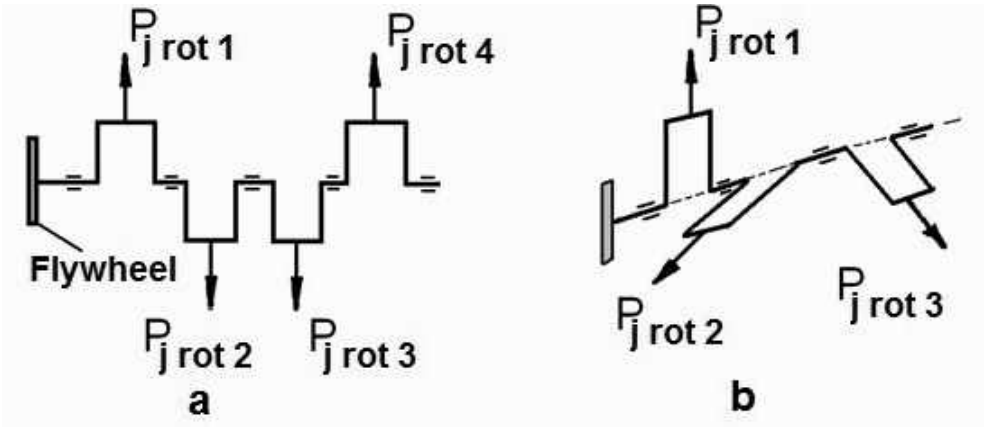

Figure 29 – Crankshafts:
a – forces of inertia and their moments are mutually balanced;
b – forces of inertia are balanced but moments of these forces are not

Same to $P_{j\,res\,1}$ the $P_{j\,res\,2}$ force cane be expressed as a projection of $\vec{C}_2$, but rotating at the doubled speed. Its absolute value is equal to

$$\left|\vec{C}_2\right| = M_n \cdot \lambda \cdot R \cdot \omega^2. \qquad (31)$$

Using the diagrams with vectors $\vec{C}_1$ and $\vec{C}_2$ for all cylinders at some definite position of the crankshaft (α) we can conclude that it is possible to provide a mutual balance of the primary and secondary misbalance of the reciprocating masses in any in-line engine. It is enough to determine the primary and secondary resultant vectors.

Example 1. Investigate the balancing state of a single row four-cylinder in-line engine.

Let us consider the positions of vectors $\vec{C}_1$ of four cylinders at zero crankshaft position $(\alpha = 0)$. Let us suppose that vector $\vec{C}_1$ of the first cylinder $\left(\vec{C}_{11}\right)$ is directed upwards (see *Figure 30, a*). According to the sequence of power strokes (1 – 3 – 4 – 2) and the crankshaft angular position $(\xi = 180°)$:

– vector $\vec{C}_{13}$ (the third cylinder) lags from the $\vec{C}_{11}$ position by 180°, i. e. directed down;

– vector $\vec{C}_{14}$ (the fourth cylinder) lags from the $\vec{C}_{13}$ vector by 180°, i. e. directed up;

– vector $\vec{C}_{12}$ (the second cylinder) lags from the $\vec{C}_{14}$ vector by 180°, i. e. directed down.

As you see, the vectors on the diagram are codirected with the crank. They cultivate the symmetrical self-balancing system. In the other words, the forces

$P_{j\,res\,1}$ acting in the single row four-cylinder engine are self-balanced.

When developing the diagram for $\vec{C}_2$ vectors of each cylinder, we must consider that secondary vectors rotate twice faster than the crankshaft. They lag from each other by a 2ξ angle, i.e. by 360° (the lag sequence matches the power stroke sequence).

The final diagram looks like in the *Figure 30, b*. Hence we can conclude that the secondary inertia in this kind of engine is not mutually compensated. The resultant force is equal to the quadruple maximal value of the $P_{j\,res\,2}$ force. It pulsates at doubled crankshaft rotational speed.

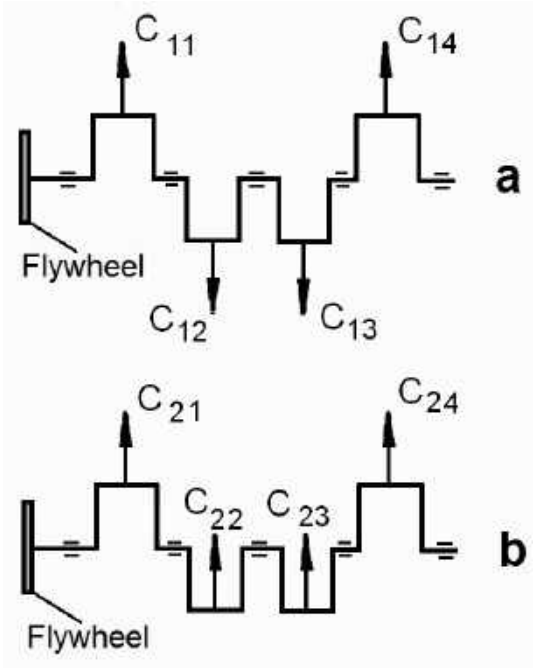

Figure 30 – Vector diagram of a single row four-cylinder engine

The Lanchester secondary mechanism is used to balance the engine of this scheme. Look at *Figure 31*. There you will see the Yamaha FJR1300 engine. The engine has the idler that rotates the counterweight at doubled rotational speed of the crankshaft.

Example 2. Investigate the balancing state of a single row six-cylinder in-line engine.

The cranks of the single row six-cylinder in-line engine lay in three planes distant from each other over 120°. The angular distance has been dictated by a $\xi = 120°$ between the adjacent ignition moments. Let us build the diagrams of $P_{j\,res\,1}$ and $P_{j\,res\,2}$ considering the operational sequence (1–5–3–6–2–4).

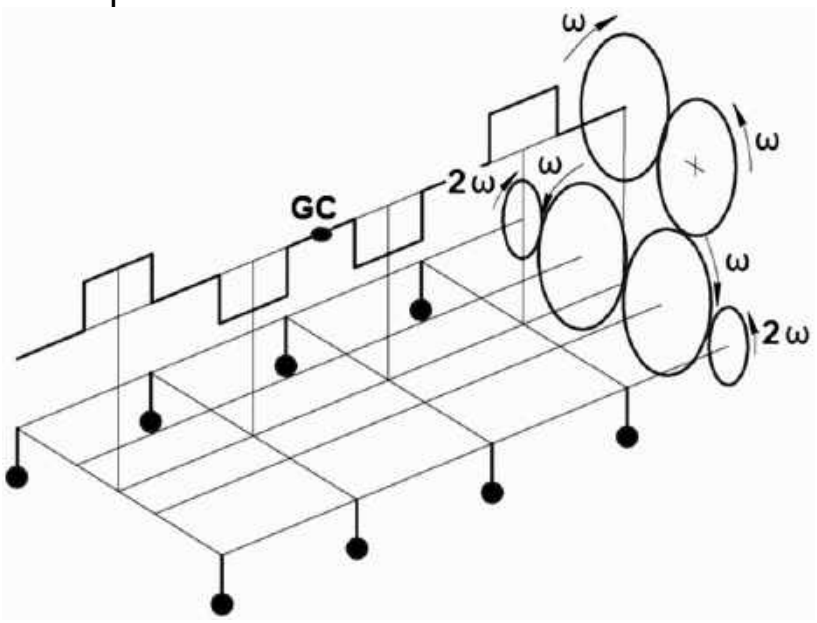

Figure 31 – The Lanchester mechanism in the four stroke engine

Remember that the $\vec{C}_1$ vectors lag from each other in the sequence by 120° (e.g. the fifth lags from the first by 120°), and $\vec{C}_2$ vectors – by 240°. Finally let us mark off them at the calculated angles (opposite to the crankshaft rotation hand, which is marked by the arrows).

The corresponding diagrams are shown in *Figure 32*. As you see, the vec-

tors are symmetrical relative to their centers. Hence, the resultant forces are equal to zeroes. It means that the primary and secondary inertia of reciprocating parts is self-balanced.

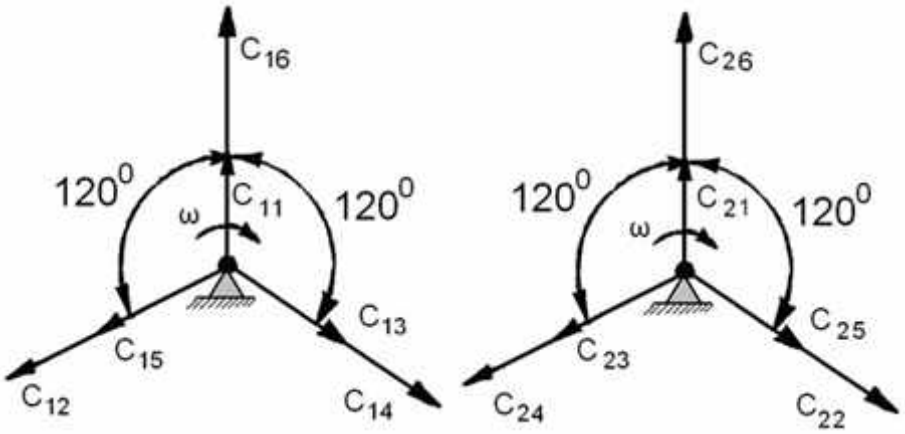

Figureure 32 – Vector diagram of a single row six cylinder engine

The $P_{j\,res\,1}$ and $P_{j\,res\,2}$ forces are balanced in a V-shape 12 cylinder engine and any other multi-row engine based on space six-crank crankshaft scheme with six-cylinder blocks.

The primary inertia of the reciprocating mass is always balanced in all single row engines. The higher order inertia of reciprocating mass is balanced only in the cases when a number of cylinders is even. Nevertheless, the moments of these forces are not balanced.

20 MATERIALS AND TECHNOLOGIES

The crankshaft is made of a heavily alloyed steel, like 18XHBA, containing nickel, chromium, tungsten. These additives make the material heavily endurant. The nitrided steels like 40XHMA are also often used.

The workpiece crankshaft is stamped. Stamping gives the optimal structure and the proper fiber arrangement, which improves the crankshaft strength for 20-30%.

The special measures must be taken for crankshaft endurance increase. For this purpose, the transfer between the main or crankpin journal and the web is made in a form of a bearing fillet. The bearing fillet of a greater radius reduces the stress concentration in the considered places, but at the same time, it simultaneously reduces the place for the bearing fitting. The transfer fillets from the webs to the webs and the edges of oil system holes (in the journals) are polished to reduce the stress concentration. Sometimes the places of the stress concentration are peened using the ball or roller knurling. The surface treatment has a great importance for endurance and a stress concentration reduction. All internal and external surfaces of the crankshaft are polished to avoid the stress concentration. The friction pairs (journals) are grinded and super finished.

The effective method to increase the endurance of the crankshaft is cementation and especially nitration (always – surfaces, usually – holes and fillets, sometimes – whole crankshaft).

21 STRENGTH ANALYSIS OF CRANKSHAFT

21.1 Endurance summary

The crankshaft is exposed to the alternating load. It is known from the experience that the material acted by the alternating load fails at stress which is not only less than the ultimate one but also less than the elastic limit.

The numerous load alternation from some minimum magnitude to the maximum one causes the progressive material degradation known as **fatigue**.

Depending on acting loads at some definite loading phase there appear the micro fractures or the conjugated fractures. Next, being acted by the alternating loads, the fracture grows and progressively occupies an increasing proportion of the section. This process finally turns into a failure. Depending on a fatigue stress range the failure development takes different number of fatigue cycles.

The fatigue cycle is parametrized with the maximum stress σ_{max}, minimum stress σ_{min}, average stress $\sigma_m = \frac{\sigma_{max} + \sigma_{min}}{2}$ and stress amplitude $\sigma_a = \frac{\sigma_{max} + \sigma_{min}}{2}$.

The limiting stress in the fatigue analysis is known as the fatigue strength. The fatigue strength is a value of stress at which failure occurs after quite a large number of cycles. The engineering experience says that the part that is not destroyed after ten million cycles will have never been destroyed, no matter how many fatigue cycles will have endured.

The fatigue strength is experimentally determined for each material and is specified in the properties of the material. The fatigue strength is determined in the reverse stress cycle. The absolute values of the maximum and minimum stress are equal in this cycle, i. e.

$$\sigma_{max} = \sigma_{min} = \sigma_a . \tag{32}$$

When the part experiences the alternating stress, its strength analysis is made using safety factors. The safety factor is a ratio of the limiting stress to the acting stress. Therefore the safety factor of any part loaded by the alternating force can be evaluated as

$$n_\sigma \cong \frac{\sigma_{-1}}{\frac{k_\sigma}{\varepsilon_\sigma}\sigma_a}; \tag{33}$$

$$n_\tau \cong \frac{\tau_{-1}}{\frac{k_\tau}{\varepsilon_\tau}\tau_a}, \qquad (34)$$

where n_σ is a safety factor of a part loaded by only the normal stress;

σ_{-1} is a fatigue strength in the reverse stress cycle (normal stress only);ъ

k_σ is a factor that considers the stress concentration due to the alternating normal stress;

ε_σ is a factor that considers the part size effect in the reverse stress cycle;

n_τ is a safety factor of a part loaded by only the tangential stress;

σ_a is a normal stress amplitude, which loads the part;

τ_{-1} is a fatigue strength in a reverse tangential stress cycle;

k_τ is a factor that considers the stress concentration due to the alternating tangential stress;

ε_τ is a factor that considers the part size effect in the reverse stress cycle;

τ_a is a tangential stress amplitude, which loads the part;

Whether the part experiences both normal and tangential stress then the common safety factor is evaluated as

$$n = \frac{n_\sigma \cdot n_\tau}{\sqrt{n_\sigma^2 + n_\tau^2}}, \qquad (35)$$

where n is a total safety factor.

21.2 Crankpin journal strength analysis

The stress in the design section of the crankpin journal can be easily determined in any crankshaft position if the crank is considered as a split cantilever beam. That means each crank is mentally split into two sections at the main bearing centers. Then the split crank is considered as a cantilever beam on two supports (*Figure 33*).

If the reactions of the supports are known then the stress in the design section can be calculated according to the following algorithm:

– the design section is mentally split;

– the parts on the left and on the right from the design sector are discarded;

– the remaining shaft part is fixed by the design section;

– the stress in the design section from the residual forces and moments (including reactions) is calculated.

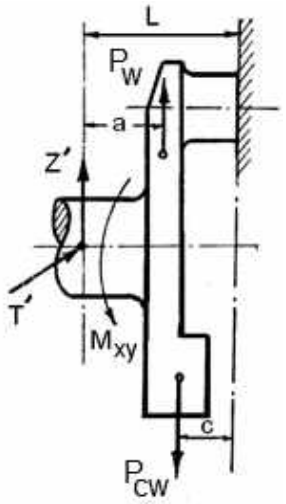

Figureure 33 – Scheme used to evaluate stress in critical points on the crankpin journal

Let us use this algorithm and determine the stress in the most dangerous crankpin journal section (*Figure 34*). It is obvious that the most stressed section of the crankpin journal is the section equally distant from adjacent webs.

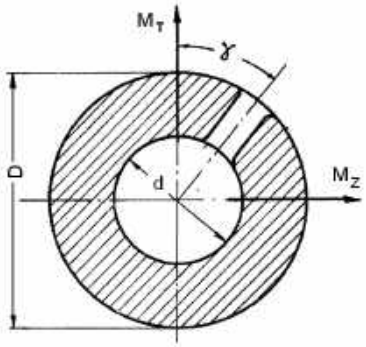

Figureure 34 – Scheme used to evaluate stress in critical points on the crankpin journal

Next, we split the journal in the middle and discard for an example the right part. Then we fix the left part on the design section and determine the stress from the residual forces and moments:

– forces acting in the crank plane (the design section is loaded with the bending moment):

$$M_{bend\,Z} = z' \cdot \ell + P_W \left(\ell - a\right) - P_{cw} \cdot c\,. \qquad (36)$$

– forces acting perpendicular to the crank plane (the design section is loaded with the bending moment):

$$M_{bend} = T' \cdot \ell\,. \qquad (37)$$

The dangerous points of the crankpin journal are near the oil feeding hole (*see Figure 29*). If the oil feeding hole is at γ angle to the crankpin plane then the bending moment in the hole plane (the plane contains the axis of oil feeding hole) is equal

$$M_\gamma = -M_{bend\,Z} \cdot \cos\gamma + M_{bend\,T} \cdot \sin\gamma\,. \qquad (38)$$

The negative sign means that the $M_{bend\,Z}$ moment causes the compression at the fuel feeding hole edge. Having determined the bending moment in the dangerous point of the crankpin journal it becomes easy to calculate the stress at this point:

$$\sigma = \frac{M_{\gamma}}{W_{bend}}; \tag{39}$$

$$W_{bend} = \frac{\pi}{32} \cdot \frac{D^4 - d^4}{D^4}, \tag{40}$$

where W_{bend} is a section modulus;

D is an outer crankpin journal diameter;

d is an inner crankpin journal diameter.

The section is also loaded with the tangential stress τ generated by the torque:

$$M_{torq} = M_{yx} + T'R, \tag{41}$$

then

$$\tau = \frac{M_{torq}}{W_{torq}}, \tag{42}$$

where $W_{torq} = 2 \cdot W_{bend}$ is a torsional section modulus.

Let us determine the parameters of the fatigue cycle as σ_{max}, σ_{min}, τ_{max} and τ_{min} and calculate the following parameters:

$$\sigma_a = \frac{\sigma_{max} - \sigma_{min}}{2}, \tag{43}$$

$$\tau_a = \frac{\tau_{max} - \tau_{min}}{2}. \tag{44}$$

Knowing the fatigue stress for the shaft (σ_{-1} and τ_{-1}) we can determine the safety factors according to the normal and tangential stress:

$$n_{\sigma} = \frac{\sigma_{-1}}{\frac{k_{\sigma}}{\varepsilon_{\sigma}}\sigma_a}; \tag{45}$$

$$n_\tau = \frac{\tau_{-1}}{\frac{k_\tau}{\varepsilon_\tau}\tau_a}. \quad (46)$$

The limiting stress of the crankshaft material is $\sigma_{-1} = 540 - 590$ MPa, $\tau_{-1} = 300 - 330$ MPa.

The stress concentration near the oil feeding holes is $\frac{k_\sigma}{\varepsilon_\sigma} = \frac{k_\tau}{\varepsilon_\tau} = 2.5$.

Knowing the safety factors evaluated by the normal and tangential stress we can determine the total safety factor by the formula

$$n = \frac{n_\sigma \cdot n_\tau}{\sqrt{n_\sigma^2 + n_\tau^2}}. \quad (47)$$

The total safety factor of actual crankshafts is within the range:

- V-shape engines $n = 1.7 - 2.9$;
- star engines $n = 3.1 - 5.5$.

Except for the safety factors in the crankpin journal, the same method is used to determine the strength in the section where the web transforms to the crankpin journal. The safety factors for these transfer regions are within the limits:

- V-shape engines $n = 1.5 - 2.6$;
- star engines $n = 2.6 - 3.6$.

21.3 Main journal strength analysis

The main journals are analyzed only on the torsion. The tangential stress in any main journal at a definite crank position is calculated as

$$\tau = \frac{M_{incomming}}{W_{torq}}; \quad (48)$$

$$W_{torq} = \frac{\pi}{16} \cdot \frac{\left(D_m^4 - d_m^4\right)}{D_m}, \quad (49)$$

where $M_{incomming}$ is a torque that incomes from the opposite to consumer end to the considered section;

W_{torq} is a torsional section modulus;

D_m is an external diameter of the main journal;

d_m is an internal diameter of the main journal.

Having determined the maximum and minimum tangential stress in the fatigue cycle (i.e. during two revolutions) we can determine the amplitude of the fatigue cycle as

$$n_\tau = \frac{\tau_{-1}}{\frac{k_\tau}{\varepsilon_\tau} \cdot \tau_a}, \qquad (50)$$

where $\frac{k_\tau}{\varepsilon_\tau} = 2.5$, τ_{-1} is a torsional fatigue strength.

The safety factors in the main journal of the existing V-shape engines is $n_\tau = 2.5 - 4.1$.

The safety factors of the star engines are high enough not to check them.

22 OPERATION AND GENERAL INFORMATION ABOUT CYLINDERS AND CYLINDER BLOCKS

Cylinder, cylinder head and piston form the above piston volume (*Figure 35*) where the air/fuel mixture is burnt. Next the evolved energy turns into a mechanical form.

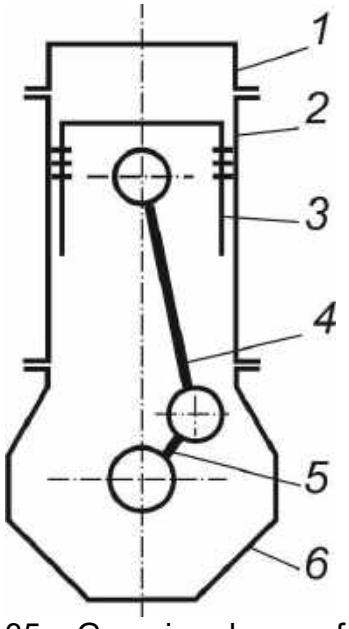

Figure 35 – Generic scheme of a piston engine: 1 – cylinder head; 2 – cylinder (cylinder barrel); 3 – piston; 4 – connecting rod; 5 – crankshaft throw (crankshaft); 6 – crankcase

Combustion happens in the upper cylinder part (the so called clearance volume). The majority of the clearance volume is formed by the cylinder head. The combustion residue at high temperature and high pressure expand in the varying volume, making the piston move.

The above piston volume remains confined while piston travels along the cylinder barrel axis thanks to a leak-proof sliding contact between the piston side surface (in cooperation with the compression rings) and the cylinder barrel. The moving piston changes the above piston volume.

Pressure of the combustion residue acts as on the piston head, so on the cylinder barrel and the cylinder head. It causes tension in the cylinder barrel along the generatrix and the cylinder head cleavage from the

cylinder barrel. At some instances it may also cause the cylinder barrel tension in a cylinder barrel axis direction.

Depending on the engine construction, the axial component of the gas force, applied to the piston head, passes to the crankcase via the cylinder barrel, a cylinder jacket (an outer cylinder shell) or an anchor tightening bolt (or a stud).

In this relation, all existing engine load-bearing frames may go into three groups (*Figure 36 a, b, c*): with the bearing cylinder barrel, with the bearing cylinder jacket or with the bearing studs.

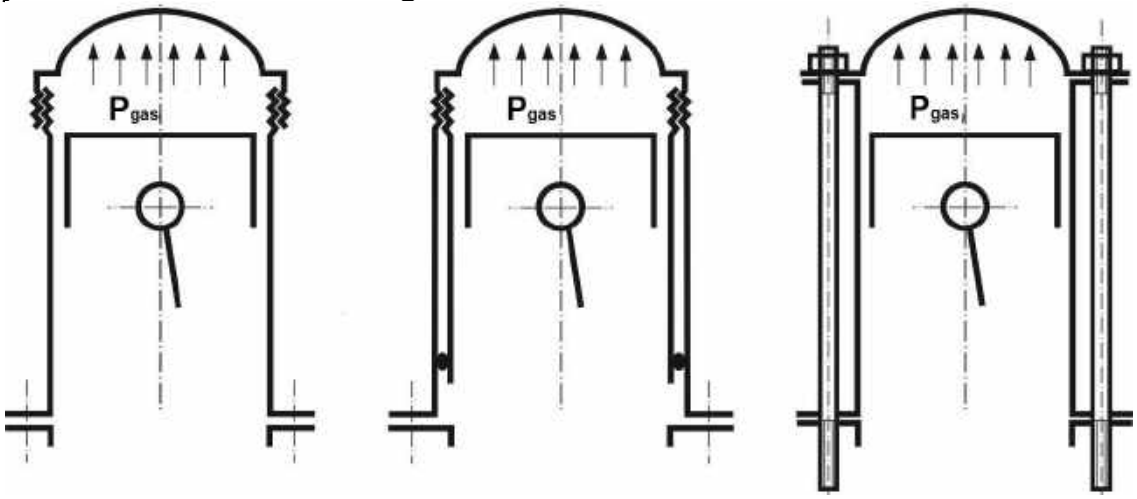

Figure 36 – Load-bearing frames of cylinder:
a – with the bearing cylinder barrel; b – with the bearing cylinder jacket;
c – with the bearing studs

The engines with the bearing cylinder barrel found its use in the air-cooled star engines. The usage of the engines with the bearing cylinder jacket or with the bearing studs is typical for the in-line and V-shape liquid-cooled piston engines.

The cylinder of the air-cooled engine is ribbed (*Figure 37, 38, b, 41*) for the cooling purposes. The air streamlines the rib surfaces and takes the heat away with it.

The main cylinder parts are:

– the cylinder head with the valves and their springs, the spark plugs and the starting valve;

– the cylinder barrel (the piston slides on the inner grinded surface also known as a cylinder bearing surface).

The cylinders of the liquid-cooled engines are surrounded with the jackets. They make up the volume, where the coolant flows and streamlines the walls of the cylinder barrel. The most abundant coolant is water.

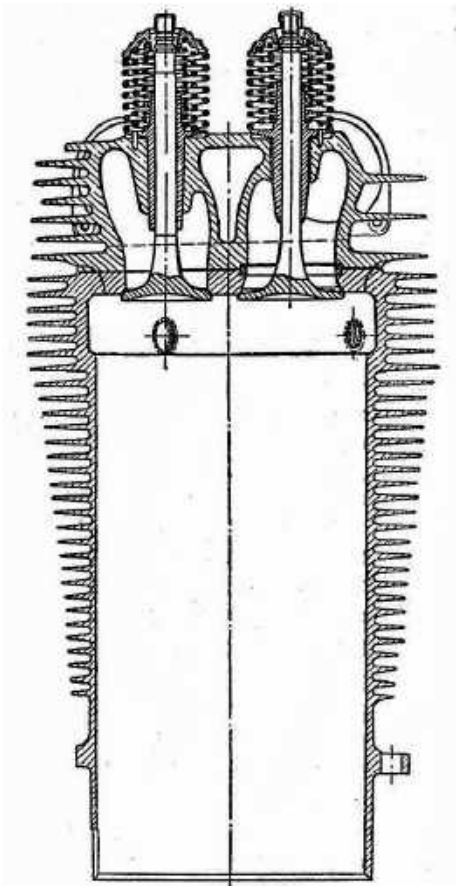

Figure 37 – Cylinder of M-22 star engine

The cylinder wall experiences both the gas pressure and the lateral force from the piston. The latest force bends the cylinder in the plane of crankshaft rotation. All these forces are time dependent. The inner cylinder wall is also heated by the hot combustion residue. The cylinder head is the most thermally loaded because the clearance volume and the channels for the exhaust gases are in this part. The cylinder barrel is less heated. The temperature state of the cylinder head is not uniform (see *Figure 38*). The region next to the intake pipe is periodically cooled with the incoming air (or air/gasoline mixture) and the region next to the exhaust pipe is periodically additionally heated with the combustion residue.

Besides, the cylinder head shape is one more source of an uneven temperature distribution because some of its regions are more cooled then the other ones. The maximum temperature drop between two points of a cylinder may reach 100 – 200 °C and the temperature of the most heated cylinder head part may reach 300 °C.

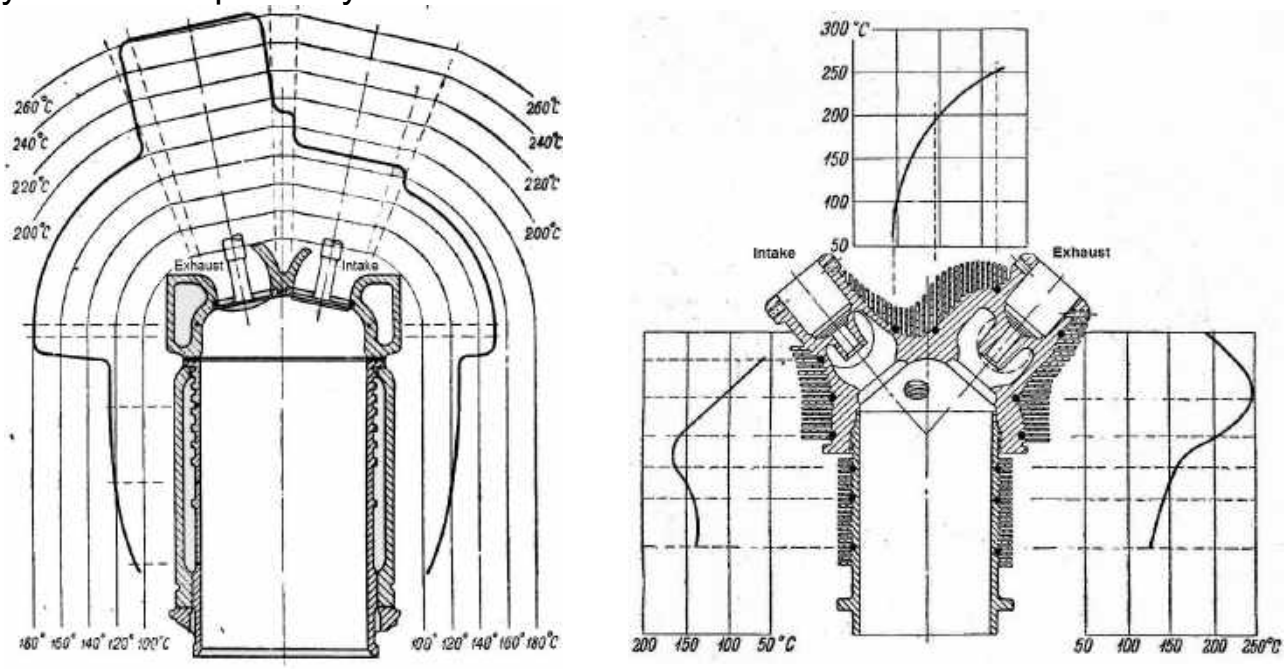

Figure 38 – Temperature field of the cylinder: a – AM-34; b – ASh-82

The uneven temperature field in the cylinder barrel and, especially, in the cylinder head results in an uneven temperature expansion of the separate re-

gions during operation. The originating thermal stresses in the cylinder head become so considerable that they usually grow more dangerous than the stress due to the pressure from the combustion residue. The thermal stress cause the warping and cracking.

Summing up all above mentioned we may conclude that the cylinder is acted both by mechanical and considerable thermal loads.

23 CONSTRUCTION OVERVIEW

All existing piston engines may be grouped by construction into:

– Engines with an individual cylinder fixation in the crankcase. The individual cylinders are in use for the star engines and the air-cooled in-line engines.

– Engines with cylinders arranged in the cylinder block, i.e. cylinders with common jacket and cylinder head. The design when the cylinders are arranged in the blocks is typical for the high-power liquid-cooled engines, e.g. VK-105, AM-42, DB-601 engines etc.

Some very old liquid-cooled engines (engines that had been producing till 1935) had their cylinders individually welded to the crankcase. The cooling jacket had been welded to each one cylinder individually. Such kind of engine (twelve cylinder V-shape engine M17) is presented in *Figure 39*. The block arrangement in the air-cooled engines is evidently impossible as each cylinder must be cooled by the flow of cooling air streamlining the cylinders.

The cylinder head is exposed to the thermal stresses stipulated by the non-uniform temperature distribution. The thermal stress become less in the case when the heat from the most heated regions, namely the exhaust valves and the bridges between the valve seats, is withdrawn more intensively.

The requirements can be fulfilled as by the intensified cooling of the cylinder head regions, so by the selecting material with the high heat conductivity (aluminum alloys) for the cylinder head.

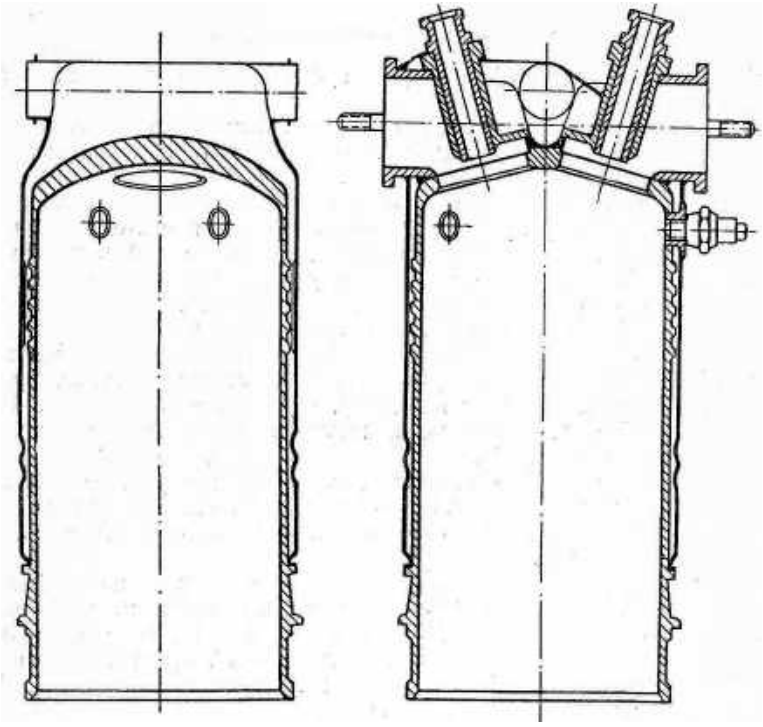

Figure 39 – Cylinder of the twelve-cylinder V-shape engine M-17

When the first method is selected then the “hot” region is more intensively supplied with the cooling agent (liquid cooling) or it is equipped with the greater

number of ribs.

The second method is of special effectiveness. Hence the cylinder heads of all modern engines are made of aluminum alloys.

Designers of the past used steel for the cylinder heads. They have an extremely non-uniform temperature field. They are more complex to be produced; getting the desired intake duct shape and combustion chamber conFigureuration becomes a real challenge of the steel cylinder head.

The aluminum cylinder head is deprived the steel cylinder head disadvantages. Aluminum is high castable. This enables the production of the intricate shape cylinder heads. The heads are rigid enough and drain the heat from the most heated regions. The aluminum cylinder heads can be casted as a single piece, the so-called a cylinder head block. The in-line engines are very favorable to have their cylinders arranged in the block. Because the distance between the adjacent cylinders becomes less, making the engine size less.

Despite some advantages of the engines with the separate cylinders, like simpler replacement and assembling, and simpler cast-out form, all liquid-cooled high power in-line engines are equipped with the cylinders arranged in the blocks.

High heat conductivity of the aluminum alloys makes the temperature field of the cylinder head more uniform and cools the cylinder head on a combustion chamber side. Hence, the heat withdrawal from the valve becomes more intense, and the air, passing next to the valve, becomes less heated. This considerably improves the volumetric efficiency and makes engine less tend towards a knocking.

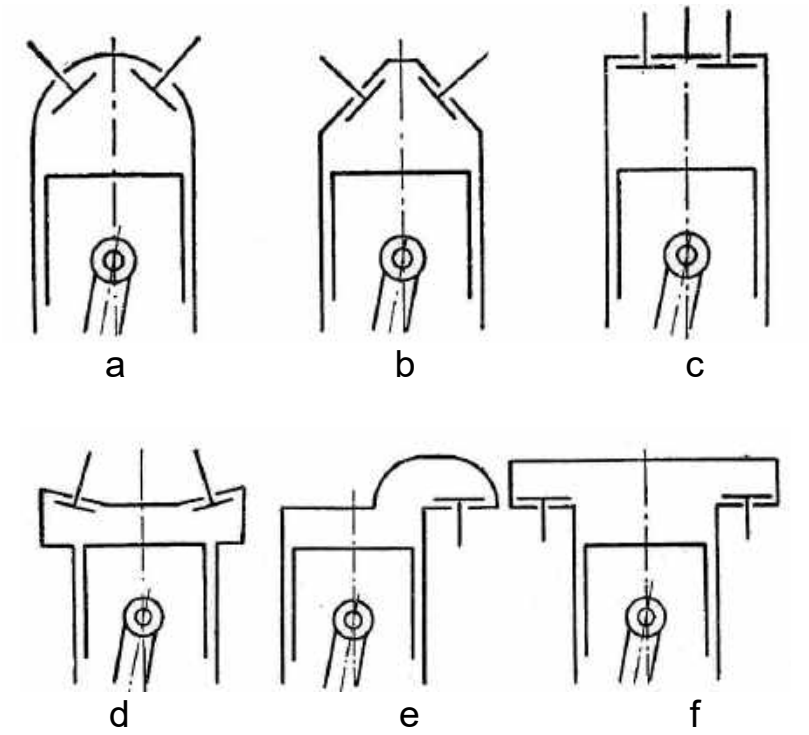

Figure 40 – Clearance volume shape:
a – hemispherical; b – spherical segment;
c – cylindrical; d – revese spherical segment;
e – L-shape; f – T-shape

The shape of the clearance volume (*Figure 40*) from the cylinder head side is selected on the set of considerations.

One of the considerations is the volumetric efficiency and, respectively, engine power. From this point of view, the clearance volume with the side valves are very inefficient (*Figure 40, e, f*). When air enters the L-shape or T-shape chamber, it must turn twice (totally – 180°), which obciously means the considerable pressure loss and, hence,

volumetric efficiency reduction. That is why the so-called valve-in-the-head chambers are used nowadays. The most abundant chamber types are hemispherical (*Figure 40, a*), spherical segment (*Figure 40, b*) and cylindrical (*Figure 40, c*).

Sometimes the clearance volume shape is changed a bit for a more convenient valve and spark plug disposition.

The cylinder head shape plays a considerable material effect on an anti-knock performance of the engine. It limits the acceptable compression ratio and the maximum pressure charging. As we know, knocking has a set of influencing factors:

- factional gasoline composition;
- mixture content;
- compression ratio;
- pressure charging;
- crankshaft speed;
- ignition timing advance etc.

But to a large extent the engine's tendency to knocking depends on the cylinder head design.

The knocking warning mission aims reducing the activation intensity of the air/gasoline mixture. The mixture activation is accompanied with the emergence of the easily degradable organic peroxides, which are the reason of the initial detonation (the volumetric air/gasoline mixture self-ignition). The activation intensity drastically grows at the increased temperature of the working substance in the zones distant from the spark plug.

Then, the structural implementation of the knocking warning mission primarily lies in the uniform cooling of the clearance volume surfaces, the hot spots elimination (they are the volumes of the earnest activation intensity) and reduction of the time required for the flame front to reach the distant volumes.

Heat conductivity of the material, of which the cylinder head is made, plays the key role for cooling of the air-cooled piston engines. This parameter expresses the material ability to transfer the heat from the hot surfaces to the cooler ones, evening the temperature of the cylinder head in this way. The effect of the unavoidable hot spots (spots near the exhaust valves and their seats) can be cushioned by fitting the spark plugs as near as possible to the exhaust valves. This approach lets the air/gasoline mixture ignition in the volumes near the valves and the cross of the strongly developing activation process here at its very beginning.

On the other hand, the knocking warning mission aims the air/gasoline

mixture combustion in the shortest possible period of time, i.e. much faster than the sufficient amount of the organic peroxide will manage to be formed. The clearance volume must be compact and free from the inactive capacities. The distance between the ignition point and the most distant chamber volumes must be as minimum as possible to break short to combustion process. To accomplish this mission the cylinders of the modern piston engines usually have two spark plugs arranged in the way to ignite simultaneously the mixture from different sides.

Outstanding results can be achieved when the mixture is swirled. The vortexes distribute the flame over the whole clearance volume generating the numerous firesides. In this case the combustion ends faster but it is more tough. The flow swirling in the specially profiled intake or in the clearance volume of a special shape has found its wide application in the automotive engines. But because of the compact clearance volume of aircraft engines, implementation of the fresh charge swirling is limited.

The combustion chamber shapes, which correspond to the highest volumetric efficiency are not considerably different from those, which correspond to the highest fuel efficiency or good anti-knocking performances.

The only combustion chambers with the highest thermal perfectness found their use in the overhead valve aircraft piston engines.

The combustion chamber perfectness can be expressed with the combustion chamber shape coefficient (CCS), which is the ratio of the combustion chamber volume V to its area A. The higher CCS is, the shorter is fire track in the clearance volume and the lower are heat losses because of the heat transfer to the cylinder wall. So, the integral indicated efficiency is also high. The best theoretical shape of the chamber is a sphere. Let us set the CCS of the hemispherical chamber equal to unity (see *Figure 40, a*), then CCS of the spherical segment is 0.99, CSS of the cylindrical one – 0.98, CSS of the revese spherical segment one – 0.96, CSS of the L-shape one – 0.93, CSS of the T-shape one – 0.85.

The position and number of the valves are selected to get the maximum channels for the gas. Besides, the designer`s decision about the valve positioning is dictated by simple and low mass valve drive.

The size of the valve heads is limited by the available place for their positioning in the clearance volume. The valve head is always round, because it is the simplest form for the production plus it provides a snug fit to the valve seat. Besides, the valve may turn round its axis during the operation keeping the snug fit to the valve seat.

The total cross-sectional area of the channel grows with the number of the valves. But big number of valves complicates the drive and valve head shape, and complicates the heat withdrawal from the most heavily heated zones of the cylinder head. That is why, even the high-speed engines have the cylinders with less than four valves (two intake valves and two exhaust valves). In case of four valves, the clearance shape is usually hemispherical or spherical segment. The hemispherical clearance volume is unfavorable in this case because the valve stems are directed to the different sides, which considerably exaggerates the valve control.

The star piston engines have the two-valve cylinder head in the vast majority of cases because their valve drives are more complicated than the drives of the in-line engines. In order to earn the broadest possible total channel, designers try to develop the valve heads of the great sizes. In this case the valves are arranged at a big included angle (up to 80°) in the hemispherical cylinder head of a big radius. Such valve arrangement provides designers with an opportunity to rib the cylinder head better, i.e. cool its central part, which is the most heated.

The valve repositioning (pay attention to the included angle) at the modification of the M-86 engine is presented in Figure 41, a, b.

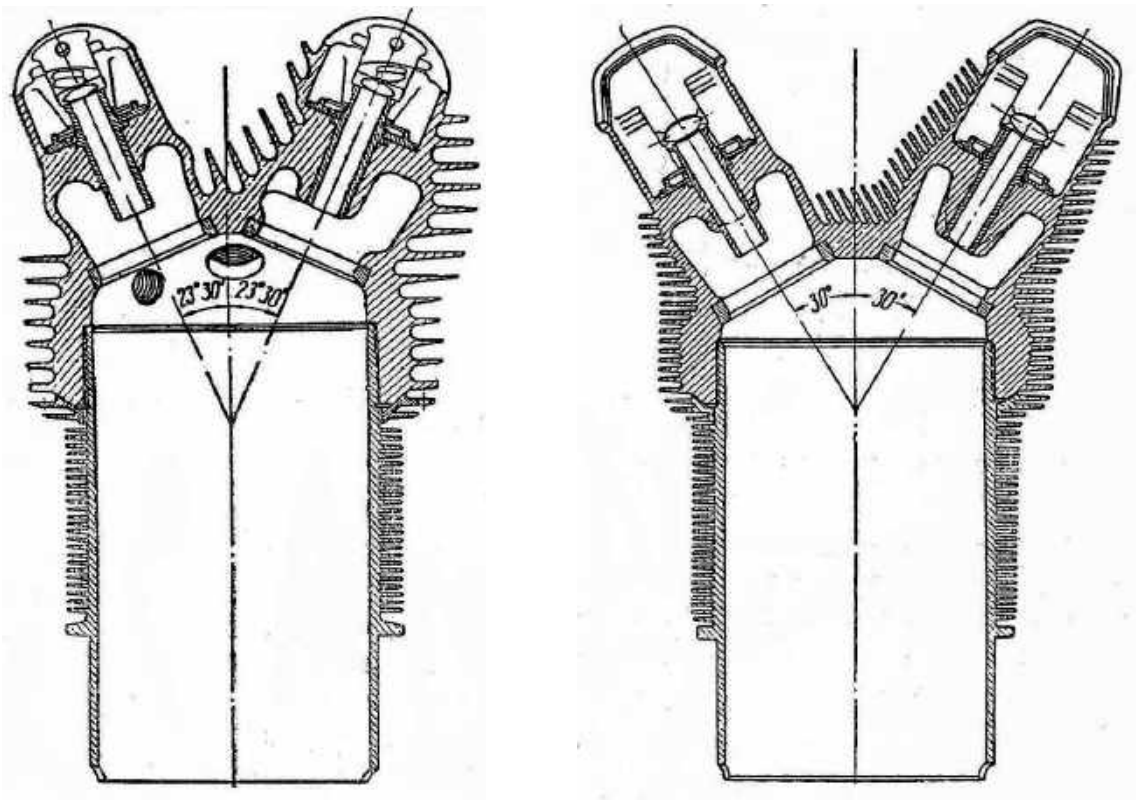

a b

Figure 41 – Cylinders of M-86 (a) and M-87 (b) engines

To shorten the time of the combustion process and to make the ignition system more reliable, the cylinder head is equipped with two spark plugs located on the opposite sides of the cylinder head walls. The first spark plug is placed near the intake valve, the other one – near the exhaust valve. The first spark plug has less hard operational conditions because it is streamlined by the cool air (air/gasoline mixture) entering from the induction channel. The second spark plug is streamlined by the hot combustion residue. Hence it is more disposed towards the overheat. Nevertheless, the spark plug near the exhaust valve is of great importance because it ignites the volumes contacting with the exhaust valve. This is a good practice to improve the anti-knocking performance.

Modern progress in piston engines aims to earn the continuous augmentation of a single cylinder power. The power augmentation is obtained thanks to the progress in the heat emission during the gasoline combustion process. But in this case designers meet another problem, which concerns the cylinder overheat (drastic temperature increase). To cope with the mentioned problem, the cooling method must provide higher cooling intensity, i.e. take more heat away from the cylinder wall. This problem can be easily solved for the liquid-cooled engines because of less heat supply to the cylinder wall and easy cooling system arrangement (the wall is always available for the water cooling). If is somewhat more complicated problem to eliminate the overheat of some cylinder head regions due to the uneven temperature field and the complex conFigureuration.

The examples of the cylinder block cooling systems are shown in *Figure 42*. In the AM-38 piston engine (see *Figure 42, b*) the coolant is supplied to the bottom of the cylinder jacket and leaves from the top portion of the cylinder head. This scheme provides good coolant circulation (from the bottom to the top) but complicates differential supply to the separate regions. In the VK-105 piston engine (see *Figure 42, a*) the coolant is supplied to the cylinder block next to the cylinder head. Then it is pumped through series of holes in the distributor manifold and is finally directed to the most heated cylinder head portion. The major portion of the coolant is taken away from the opposite side of the cylinder head. The lack of this cooling scheme is the limited coolant circulation near the cylinder barrels. The same coolant supply system is provided for the DB-601 piston engine with the inverted cylinder block (*Figure 42, c*). But in this case, the fluid drainage is provided from the upper cylinder block portion, i. e. from the cylinder jacket near the piston skirt at TDC position.

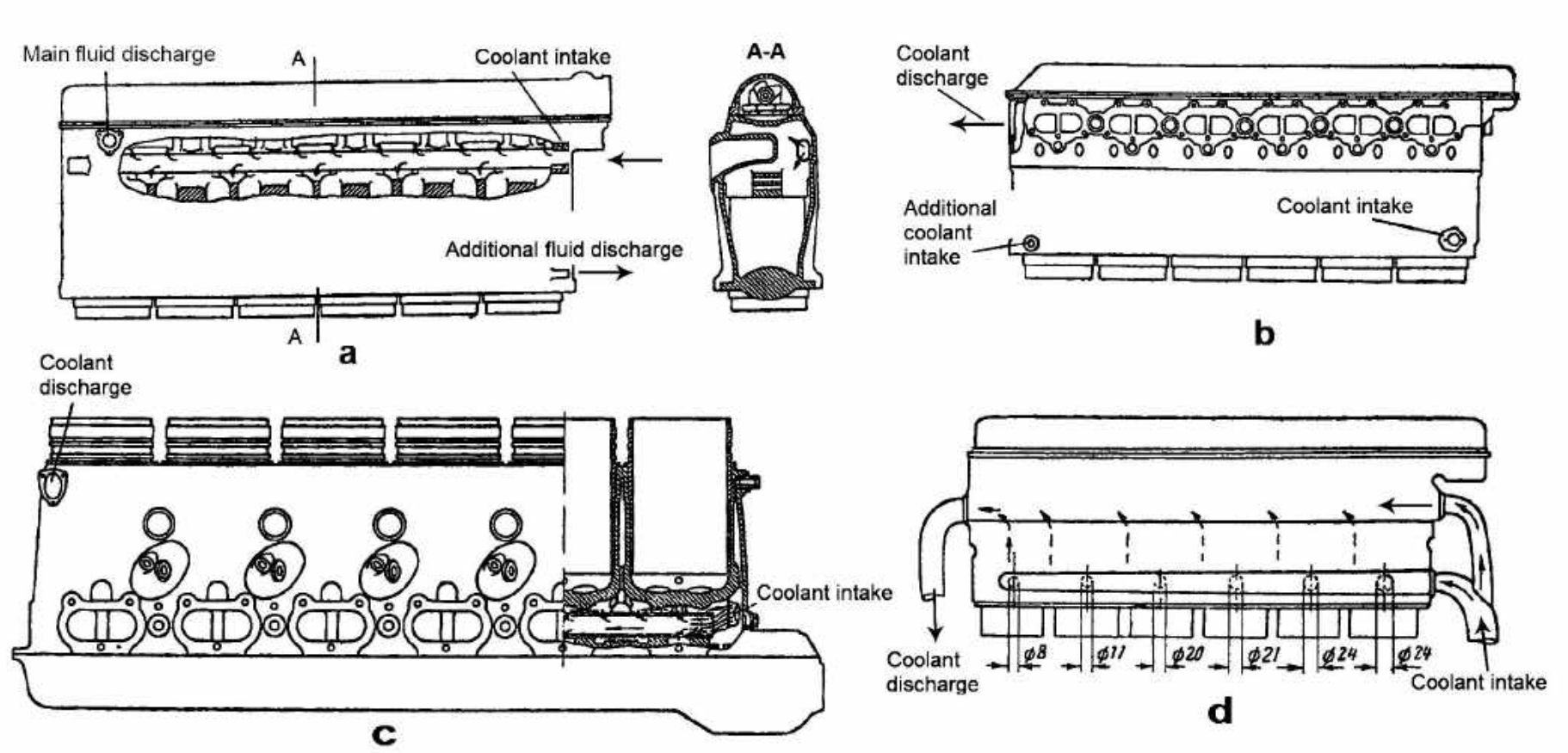

Figure 42 – Cylinder block cooling

An engine with the cylinder block like in *Figure 42, d* has its coolant simultaneously supplied to a cylinder block bottom (near the barrels) and to its top (near the cylinder head). The coolant intake of each cylinder (sizes and position) is experimentally determined to make the temperature field of the separate cylinders uniform. The barrels of the liquid-cooled engines may be wet or dry (see *Figure 39*). The barrel is considered wet in case it is mounted inside the cylinder block and is streamlined with the coolant. The barrel is dry in case it is pressed in the cylinder block jacket along the full length. The dry steel (cast iron) barrels are not cooled with water directly, but through the aluminum jacket. The dry barrel design has high rigidity and strength, small cylinder strains. It does not need the butt between the barrel and the jacket to be sealed. The disadvantage of the dry barrel is its increased temperature and the worse heat withdrawal because of an extra wall between the barrel and the coolant. The aluminum and cast iron barrels are widely implemented in the land application engine building. The cylinder bearing surface of the cast iron barrels is bored. The cylinder bearing surface of the aluminum barrels is also bored, but next it is covered with the special materials. The problem of air-cooled piston engine cooling is solved by the sufficient enough heat exchange area (ribbed surface).

The cylinders of the M-22, M-86 and M-87 engines are shown in Figures. 37 and 41. As you may see, the cylinder of M-22 piston engine, produced at late 20-ies of the XX^{th} century, had the steel barrel bottom and the poorly ribbed head. The cylinder of M-86 piston engine (see *Figure 41, a*), produced much later, had an aluminum barrel bottom and more advanced ribbed head. The cylinder of M-87 piston engine is of the same diameter as M-86 (see *Figure 41, b*). But its power is considerably greater. Hence it has 40% more ribbed surface against the prototype.

Cylinders of more modern air-cooled engines, like ASh-82, have even more advanced ribbing (see *Figure 48*).

The ribbed area to cylinder volume ratio (RACV) characterizes the ribbing degree. The specific RACV mostly depends on the distance between the adjacent ribs (i.e. on a rib pitch) and on their length. The rib pitch of modern steel barrels is 3 – 4 mm (aluminum barrels – 5 – 6 mm). The rib length of the steel barrel is 14 – 18 mm. For some regions it may amount to 55 – 65 mm. The modern air-cooled engines of high power have the specific RACV equal to $0.8\ \frac{m^2}{litre}$. The ribbed area to engine power ratio may amount to $1.9-2.7\frac{m^2}{kW}$. The further increase in RACV by means of the smaller rib pitch or the longer ribs is constrained because of the manufacturing considerations and less efficient cooling. It becomes quite hard to feed the rib root with the air and the rib tips become overcooled. The maximum reasonable rib length of the steel ribs is much less than of the aluminum ones.

In the case of the high power star engine, the most of heat (60 ... 70%) must be withdrawn from the cylinder head. So, its surface is 2-2.5 times more

ribbed than the surface of the barrel. The cylinder head ribbing is not symmetrical, because it depends on the temperature field. For example, the region of the exhaust valve must be more ribbed than the same region of the intake valve. The longest ribs are in the region between the intake and exhaust manifolds, right above the middle of the combustion chamber. Sometimes the deflecting is implemented in order to uniform the temperature in the separate regions of the head and the sleeve. The deflecting constitutes the dashboards, directing the air flow to the most heated cylinders or head parts.

The limited surface available for an efficient cooling in the conventional designs of the air-cooled cylinders has tended to the attempts to increase the barrel height where the ribbing implementation is reasonable. This became the reason for the introduction of aluminum ribs with high thermal conductivity (*Figure 43*).

A sort of ribbing can be manufactured as single or twin ribs rolled into the steel barrel (*Figure 43, a*), or as an aluminum ribbed jacket pressed on the smooth steel barrel (*Figure 43, b*).

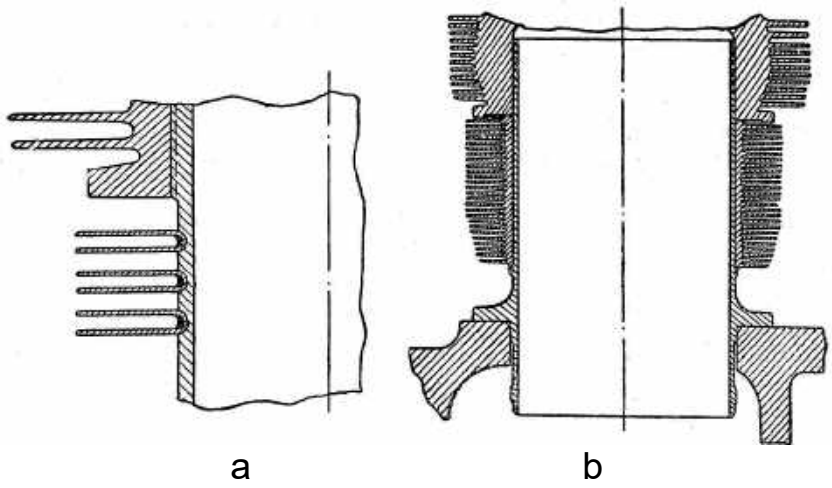

Figure 43 – The scheme of barrel with aluminum ribs cooling: a – rolled ribs in the steel barrel; b – pressed on the aluminum barrel

It is observed that the aluminum ribbing effectiveness mostly depends on the thermal state of the contact between the ribbing and the barrel.

In other words it depends on a fit tightness and contact quality, which in their turn depend on production and assembling methods. So, for example, the pressing of the aluminum jacket on the steel barrel may not provide the full-length contact in the case the contacting surfaces had been treated to be the 6^{th} class of accuracy (see *Figure 43, b*). Of course the heat exchange between the barrel and the ribs becomes worse.

The issues in the cylinder barrel production (especially their heads with large ribbed area) make designers of the engines with low power-to-displacement ratio give preference to the cylinder heads with less ribbed area.

One of the most crucial, sometimes difficult to achieve tasks to be solved while designing the cylinder assembly is the gastight joint of the barrel and the cylinder head. The so-called gas seam must eliminate the gas breakthrough.

The water-cooled engines with cylinders arranged in blocks have their gas seam sealed by the pressed barrel`s top shoulder to the cylinder head in two ways:

– by tightening the threaded bolts (see *Figure 46*, the M-38 engine);
– by screwing the barrel to the block with negative axial clearance (see *Figure 47*, the VK-105 engine).

In both cases, the contacting face surfaces of the barrel and the head are equipped with the cylinder-head gasket made of soft material (annealed copper or aluminum, the AM-38 engine) or harden steel (corrugated ring, the VK-105 engine) for better seam sealing. The construction of the modern cylinder-head gaskets is shown in *Figure 44*. When engine is heated up, the negative clearance becomes 40–60% less due to greater thermal expansion of the aluminum cylinder head against the steel barrel. So the “cold” negative clearance is enlarged to compensate the heating. The special profile and high precision of the thread on the head and sleeve is one more source to improve the sealing quality.

One more option for the gas tightness is the cutting-in of a “special tenon” of the steel barrel into the aluminum cylinder head followed by its locking (*Figure 45, a*) or its screwing with negative clearance (*Figure 45, b*).

The joint between the cylinder and the crankcase depends on an engine construction and the cylinder arrangement. For example, each separate cylinder of a star air-cooled engine is studded to the crankcase individually via the flange of the steel barrel. From 10 to 16 studs are screwed in the crankcase (see *Figure 46*).

Thus, the force of the gas pressure, breaking the cylinder away from the crankcase, comes to the latest through the sleeve and the mounting studs.

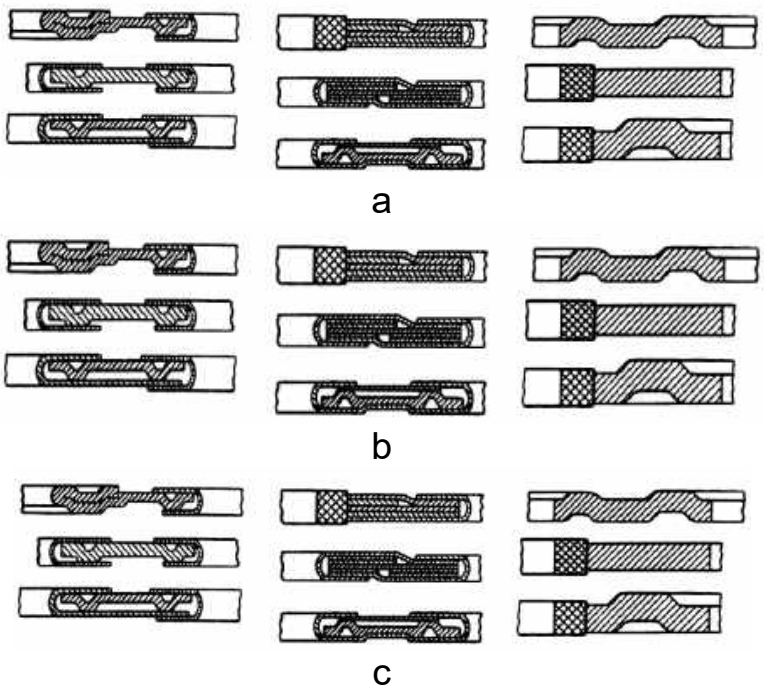

Figure 44 – Cylinder-head gaskets:
a – metallic; b – combined with the screening rings; c – combined with the elastic edges

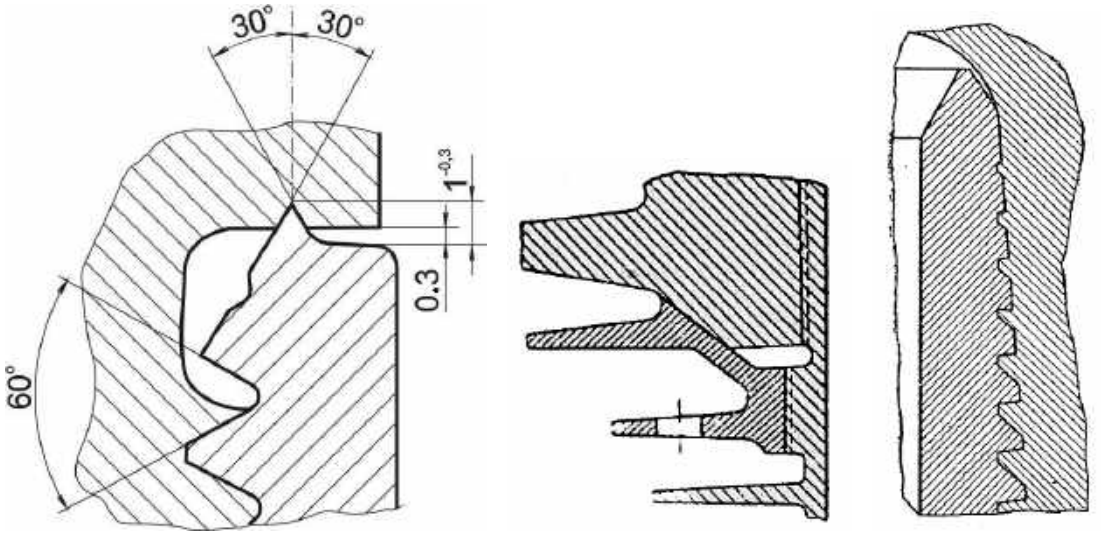

a b

Figure 45 – Methods to seal the joint between the cylinder and the crankcase:
a – cutting-in of a “special tenon” of the steel barrel into the aluminum cylinder head followed by its locking; b – interference by the effective thread diameter

If the cylinders are arranged in blocks then each cylinder is not fastened individually, but the entire block is attached. Two methods show themselves good in the maintenance and became widely used. In the first case the cylinder block is fastened to the crankcase with the short studs by the bottom flange of the cylinder block jacket (see *Figure 13*). The force of the gas pressure (the force alternates from zero to the maximum value) gets to the crankcase via the jacket of the casted aluminum block. Hence, the jacket must have the rigidity and strength enough, i.e. the jacket must be thick-wall (8–10 mm).

In the second case, the cylinder block is fastened to the crankcase with the long power studs and nuts resting against top cylinder head surface (see *Figure 46*). The jacket of the cylinder block is preliminary compressed while assembled (during the studs tightening). The tension by the gas pressure gets to the crankcase via the studs, so, being acted by the tension, the jacket is somewhat unloaded. Such operational conditions are more favorable for casted aluminum parts against the ones with the alternating tensile force (the first case). Moreover, one more advantage of the second case is the convenient maintenance. The barrel can be easily changed in maintenance.

The cylinder block can also be fasten to the crankcase with the nuts and the cylinder liner part projecting into crankcase (DB 600 series engines). But this method became less favorable one due to the complex assembling and disassembling.

24 EXAMPLES OF CYLINDER BLOCKS

24.1 The M-38 engine

The cylinder block consists of six cylinders arranged in a row, a separate cylinder head and a separate cylinder jacket (*Figure 46*). The two latest are

produced of a thermally treated aluminum alloy.

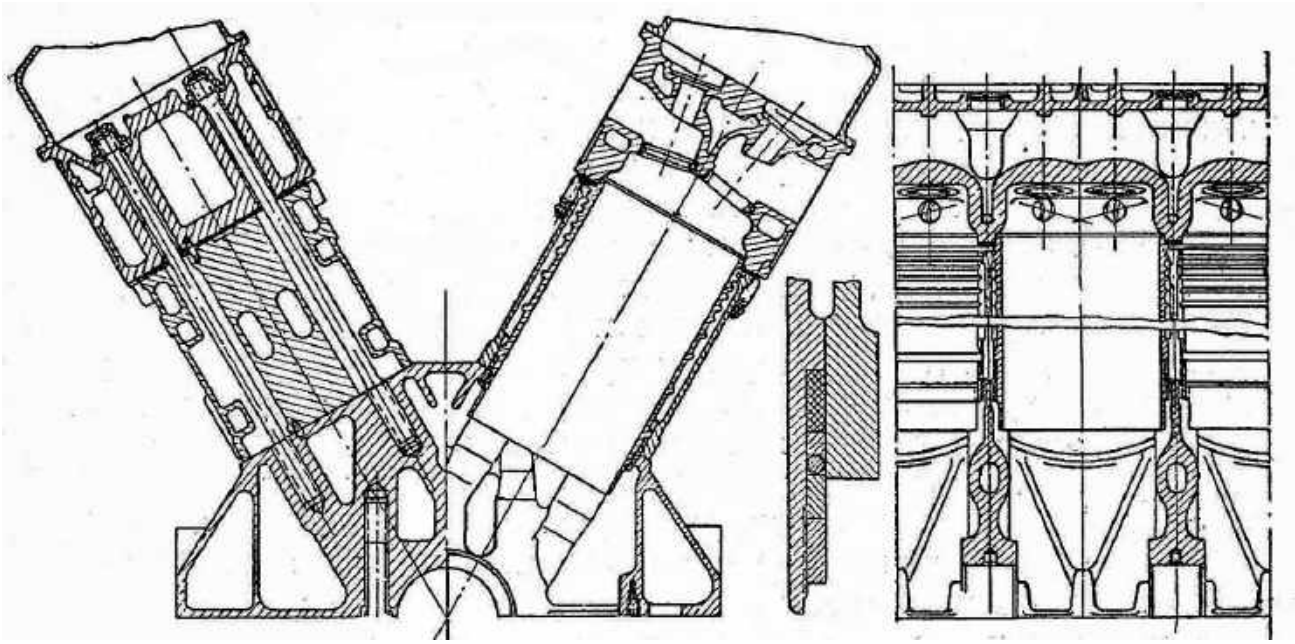

Figure 46 – Cylinder block of the AM-38 piston engine

The steel cylinder barrel is loosely fitted in the cylinder jacket from above. Its upper shoulder is enclosed between the cylinder head and the cylinder jacket. The cylinder block is studded to the crankcase by fourteen long power studs. They simultaneously mutually join the cylinder head with its jacket and reliably seal the gas seam between the face surfaces of a barrel flange and a cylinder head boring. For more reliable joint, the gas seam between the cylinder head and the barrel flange has a copper cylinder-head gasket. The cylinder jacket gets clamped between the cylinder head and the crankcase while the studs become tightened. In this case, as it was considered above, the force of the gas pressure gets to the crankcase through the power studs, compensating the jacket`s compression. The constrained only by the top flange cylinder barrel takes zero axial forces. Hence it will be able to strain freely when the temperature changes.

The rubber and steel rings on the barrel`s bottom part seal the water volume between the barrel and the jacket. The steel ring lines with the bottom ring while mounted. These assembly is tightened with a nut.

Except the fourteen power studs, the cylinder block head is additionally studded with auxiliary studs, who even the butt tightening and facilitate the cylinder block fitting on the crankcase.

The spherical segment combustion chamber has two exhaust and two intake valves. Their axes are tilted at some small angle regarding the cylinder axis.

Above the valves one can find two longwise fitted camshafts. The first one actuates the intake valves of each cylinder, and the other one – all exhaust valves.

Steel valve seats are pressed in the cylinder head with the considerable negative fit. The intake valve seat is pressed on a conical surface, the exhaust one – on a cylindrical surface.

Each combustion chamber contains three apertures for two spark plugs and single kickoff valve (for a compressed air start).

The cooling water is supplied in the bottom of the cylinder block jacket. Then is travels up till it meets the apertures between the jacket and the cylinder head. After all it gets through these apertures inside the cylinder head. The joints between the jacket and the cylinder head are sealed with rubber rings in the places of the overflow apertures. The coolant fills all the cylinder head volume (the volume between the combustion chamber wall and the induction and exhaust manifolds and an outer cylinder head wall). Finally, the worked out coolant is drained through the hole in the front top region of the cylinder head.

24.2 The VK-105 engine

Unlike the AM-38 cylinder block, the six-cylinder cylinder block of VK-105 has its cylinder head and its jacket casted together (*Figure 47*). This design eliminates the problems with the gas seam and the joint for coolant overflow. So the engine does not need the set of fasteners and seals anymore. The cylinder block becomes more rigid but the casting process and the barrels fastening grow much complex. The barrels are screwed in the sockets of the cylinder block, which are at the bottom of the combustion chamber. The screw is simultaneously sealed in two ways:

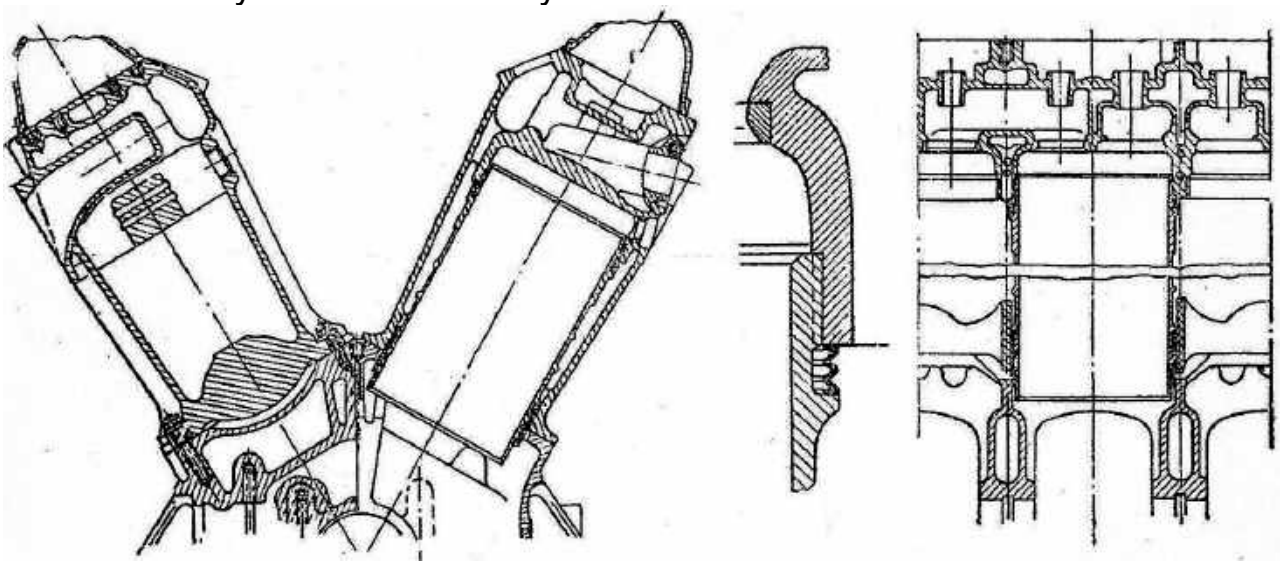

Figure 47 – Cylinder block of the VK-105 engine

– the barrel is screwed with negative clearance in the cylinder block (to prevent the screw tear, the barrel must be screwed in the preliminary heated cylinder block);

– fitting the special elastic steel sealing bands between the top barrel`s flange and the face of the cylinder block socket.

Same to the AM-38 engine, the barrels are constrained only by the upper shoulder. They can elongate freely when the temperature grows. The sealing of a coolant path is the same to the AM-38 (AM-42) engine. The barrel fastening in the cylinder block with the interference screw makes assembling and disassembling to be hard tasks. The assembled cylinder block is fitted on the crankcase with 42 short thread studs. Big number of studs and a rigid flange in the bottom of the cylinder block secure the uniform butt tightening. There are three valves (two intake and single exhaust valves) in the bottom part of the combustion chamber. All manifolds for mass exchange and, hence, all pipelines are from the outer side of the cylinder block giving free space for a quick-firer with a coaxial to the crankshaft axis muzzle. All valves are actuated through the single camshaft, which rests in the bearings on the top of the cylinder block. But for all that, opposite to the exhaust valves that are directly actuated by the cams, the intake ones are actuated via the cross-arms. The guides of the cross-arms are fixed in the cylinder head.

Cooling water is fed to the top cylinder block`s part through a pipe in the cylinder head. The pipe has a collection of radially arranged holes, which, above all, guide the water streams to the most heated cylinder head regions. The water inside the jackets moves mostly because of convection. The water is drained from the cylinder block through the holes in the top part of the cylinder block, namely near the pipe. Besides, the water is partially drained from the bottom part of the jacket via an external pipe. This water bypasses a radiator and gets to a water pump. The same pipe also serves for a water drain from the cylinder block.

24.3 The ASh-82 engine

The ASh-82 engine is a high-power 14 cylinder air-cooled star engine (see *Figure 48*). Each cylinder is a separate standalone structural assembly, which is fitted on the crankcase individually. The cylinder is an assembly consisting of a steel ribbed cylinder barrel and a heavily ribbed aluminum cylinder head. The cylinder head is screwed in the cylinder barrel. Outside the thread one may find the centering collar.

As it has been mentioned above, the gas seam sealing is arranged by the interference on the centering collar and on the thread between the cylinder head and cylinder barrel. The “cold” interference fit is equal to 0.45-0.55 mm. When the engine is warming up, the clearance slightly decreases.

To facilitate the cylinder barrel screwing in the cylinder head, the latest one is heated up to 300 °C. The thread on the barrel`s surface is notch-shaped to provide additional sealing of the gas seam.

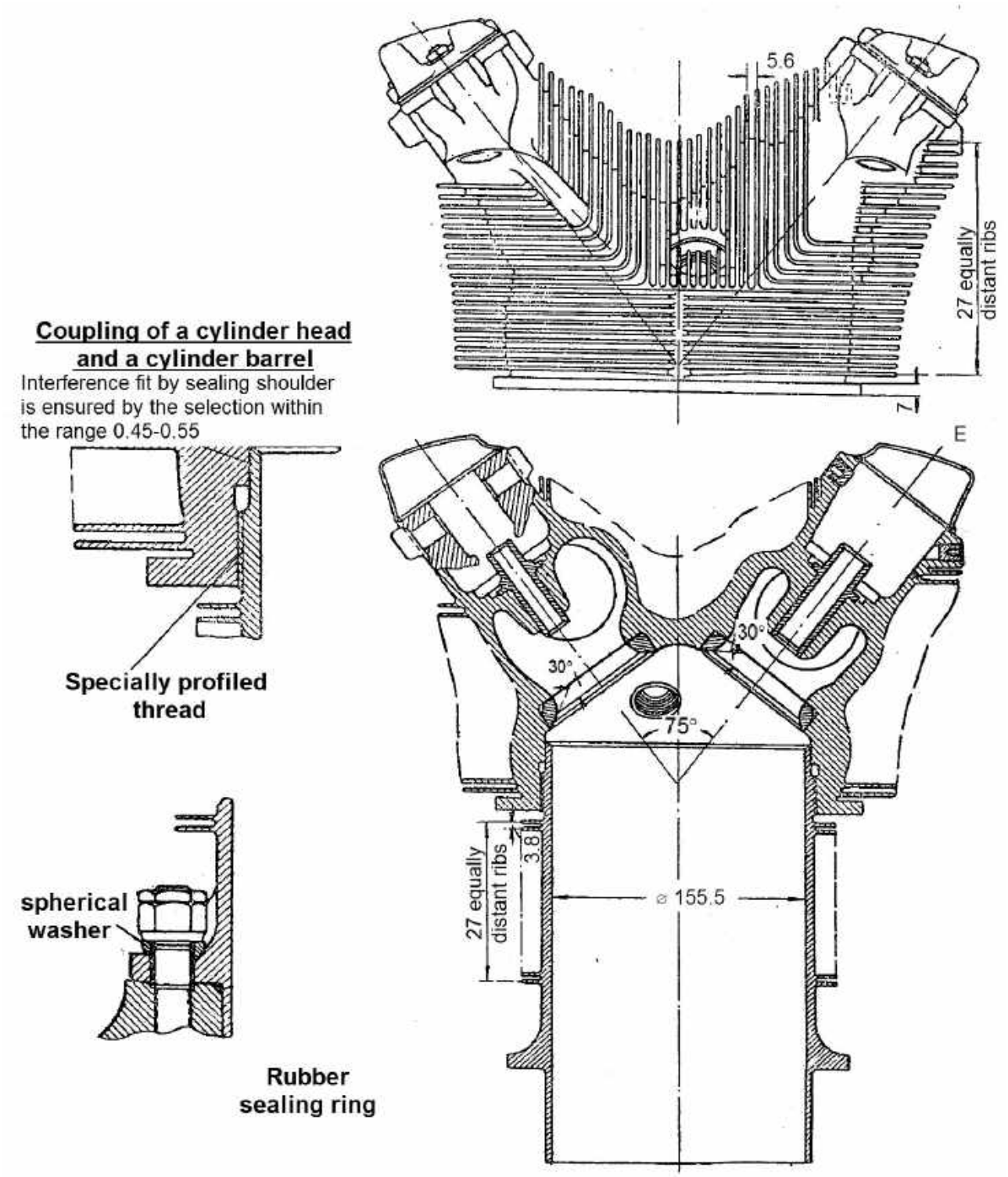

Figure 48 – Cylinder and head of the ASh-82 engine

The thread experiences the considerable force while the fuel is being combusted. The distinguishing feature of the buttress thread is an absence of the radial component of the force, which would burst the nut (in our case the nut is a cylinder head) and would compress the bolt (in our case the bolt is a cylinder barrel). In this meaning the used thread is similar to a flat thread but is different thanks to the higher strength. The couple of the last thread turns are usually negated giving better gas tightness of the gas cavity.

The cylinder is studded to the crankcase with the flange in the bottom of the cylinder barrel. It means that the force of gas pressure gets to the crankcase through the cylinder barrel, thereby loading it with variable in time tensile force. The barrel has 27 dented ribs (the pitch is 3.8 mm, the length is 14 mm). The overall area of the ribbed surface of the cylinder barrel is 5100 sm^2. The overall area of the ribbed surface of the cylinder head is much higher. It takes about 12200 sm^2. The ribs at combustion chamber level are horizontal. Besides, to minimize the non-uniform temperature distribution on the cylinder head, the rib length on the intake valve side is less than on the exhaust valve side.

The cylinder head contains two valves mutually tilted at an angle 75° (one intake and one exhaust valve).

25 MATERIALS AND PRODUCTION

Cylinder blocks (jackets and heads) of liquid-cooled engines are casted with the following thermal and mechanical treatment. They are made of aluminum alloys AL4 and AL5.

Cylinder heads of the air-cooled engines are casted of aluminum alloy AL10, which high-temperature strength is higher than of AL4 and AL5. Nowadays, the cylinder heads of some air-cooled engines are stamped or forged of aluminum alloy AK2 and then – chemically treated. The stamped aluminum alloys have higher mechanical properties than the casted alloys. Besides, stamping almost eliminates the probability of pockets, porosities or internal cracks that are very common for the casted cylinder heads. The main trouble heading toward the stamped cylinder head implementation is high labor expenditures on machining. This trouble is partially eliminated by a modern, more perfect production process. The stamped and next mechanically treated cylinder heads may have 15 – 20 % greater ribbed surface than the casted cylinder heads.

The cylinder barrels are made of a special nitrogenized steel 38ХМЮА or lean alloy steel (σ_u = 850 MPa). The opportunity to implement the lean alloyed steel for the cylinder barrels appears thanks to the low acceptable stress, which in its turn caused by designers` wish to reduce the barrel straining. The cylindrical bearing surface must be carefully treated to bring the wear and friction down. To get the high-quality surface it is honed. The cylinder bearing surface of the most cylinders (AM-38 and ASh-82) is nitrogenized for a less wear out. To protect the barrel surfaces that are in contact with the cooling water from corrosion they are additionally coated (usually it is cadmium plating). The most stringent tolerances in the machining of parts of air-cooled cylinders are made to the elements of the “head–barrel” coupling, as well as to the cylinder bearing surface profile. The tolerances of the connecting belt cover both diametric dimensions of the centering cylindrical surfaces and other elements, including the thread profiles (pitch diameter, outer and inner diameters, pitch, profile angles, rounding radiuses). The machining tolerances address as the diametrical

sizes, so probable roundness and taper of the cylinder bearing surface profile. The tolerances are assigned on 4-5 quality class.

The manufacturing process of the cylinder barrel must consider a probable distortion of the bearing surface at the top, caused by the barrel pressing in the cylinder head. The bearing surface is also distorted during operation because of uneven temperature field along the cylinder barrel length. So, considering the temperature non-uniformity, most engines have their cylinder barrels profiled to be a bit different from cylindrical. Their “cold” shape is selected in the way to be transformed to the cylindrical one at operational conditions. Cylinder shaping in this case requires a very accurate analysis of temperature strains at different zones of the cylinder barrel. The upper zone is commonly conical, i.e. the diameter diminishes for 0.1-0.3 mm to the combustion chamber side.

The specific requirements to a mechanical treatment of the cylinder blocks of the liquid-cooled engines purpose making all barrels of the block coaxial and minimizing the barrel`s shape distortion, as you remember, caused by a barrel fitting in the cylinder block.

The fitting studs, especially long power studs that are considerably loaded, are manufactured of high-alloy steels, like 18XHBA. The thread is the most weak point of the joint. To make the thread of the studs more strong, it is manufactured at extremely careful level; sometimes it is specially profiled (with a greater rounding radius of the inner thread diameter).

The stud body is grinded and next polished. The transfer from the body to the thread is designed in a form of a smooth fillet. The fillet is of a big radius to eliminate the stress concentration. The fillet is also polished.

26 STRENGTH ANALYSIS

The strength analysis of the cylinder assembly and its parts (especially cylinder block head and jacket) cannot be made analytically, even with great number of assumptions, because shape of the parts is very complex. But, the analyses like this can be performed in modern CAE programs like ANSYS. Next in the manual you will see some very simplified analyses of some parts from the cylinder assembly.

26.1 Cylinder wall strength analysis

Cylinder walls are analyzed on tension being acted by the gas pressure. The tension occurs as along the transverse (annular) cross-sections so in the center plane (along a generatrix). The tension along the transverse cross-sections happens when the force of the gas pressure gets to the crankcase by the cylinder barrels. This is the truth for air-cooled engines. The break in the center plane of the air-cooled cylinders is less probable, as the wall is enhanced by the ribs.

The maximum excessive gas pressure that was obtained by air/gasoline mixture combustion serves as a design pressure in the analysis.

If the minimum cylinder wall thickness above the flange is δ' (*Figure* 49) then a tensile stress σ'_{tens} in a ring cross-section is

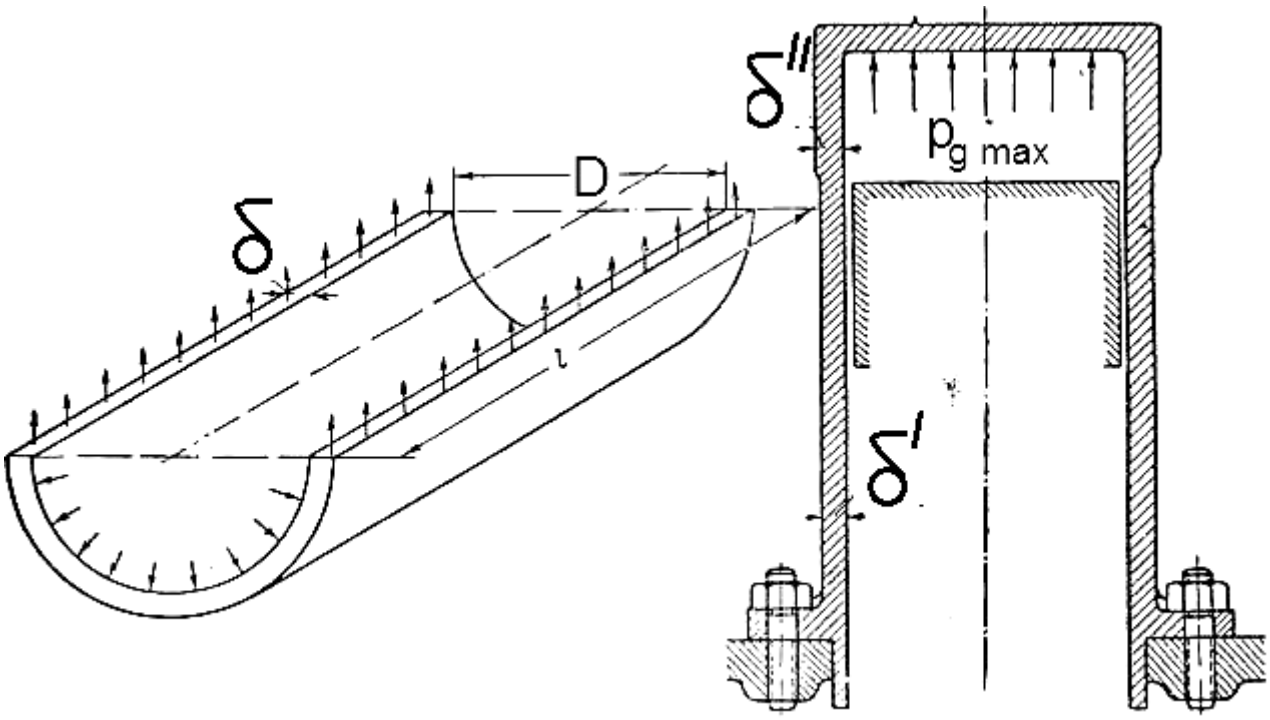

Figure 49 – For the cylinder wall strength analysis

$$\sigma'_{tens} = \frac{\left(p_{g\,max} - p_{atm\,des}\right)\frac{\pi D^2}{4}}{\pi D\delta'} = \frac{\left(p_{g\,max} - p_{atm\,des}\right)D}{4\delta'}, \qquad (51)$$

where $p_{g\,max} - p_{atm\,des}$ is the maximum excess gas pressure in the cylinder;

D is a cylinder diameter.

The force tensing the cylinder along the generatrix is

$$F''_{tens} = \left(p_{g\,max} - p_{atm\,des}\right)DL \qquad (52)$$

where L is the length of the generatrix.

It initiates the corresponding stress:

$$\sigma''_{tens} = \frac{\left(p_{g\,max} - p_{atm\,des}\right)DL}{2L\delta''} = \frac{\left(p_{g\,max} - p_{atm\,des}\right)D}{2\delta''}, \qquad (53)$$

where δ'' is a design cylinder wall thickness.

Hence, if the walls are of the same thickness $(\delta' = \delta'')$, then the tension in a ring cross-section is two times less than the tension along the generatrix. But the maximum pressure elongating the cylinder along the generatrix acts only on the top part of the cylinder barrel (region of the combustion chamber).

That is why not the minimum wall thickness must be inputted in the equation (53) but the wall thickness in the top cylinder`s part δ'', which is usually greater than δ' (see *Figure* 49).

The stress from equations (51) and (53) must not exceed 110 MPa. The relatively low limiting stress explains necessity to have the thick wall to ensure enough rigidity.

26.2 Cylinder barrel flange strength analysis

The flange is analyzed on bending being acted by the maximum force of the gas pressure $p_{g\,max}$. According to the scheme in *Figure* 50, the acting bending moment can be esteemed as

$$M_{bend} = P_{g\,max} \cdot b, \qquad (54)$$

where $P_{gmax} = \left(p_{g\,max} - p_{atm\,des}\right) \cdot \pi \cdot D^2 / 4$.

The section modulus is evaluated as (the design section curvature is neglected)

$$W_{bend} = \frac{\pi d a^2}{6}, \qquad (55)$$

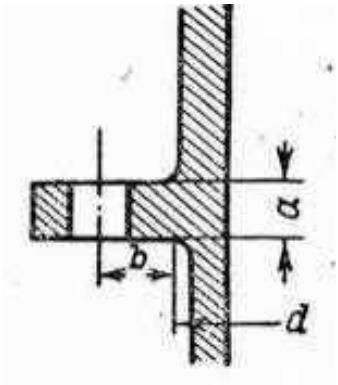

Figure 50 – For the cylinder wall strength analysis

whence bending stress is

$$\sigma_{bend} = \frac{M_{bend}}{W_{bend}} = \frac{6P_{g\,max} \cdot b}{\pi \cdot d \cdot a^2}, \qquad (56)$$

where σ_{bend} must not exceed 120 MPa.

26.3 Studs strength analysis

This analysis addresses the studs joining the cylinder with the cylinder block. They are analyzed on a breakaway being acted by the pretension. The pretension is 25 % greater than the force of the maximum gas pressure, which is enough to be sure that the seam will not fail. The inner diameter of the thread is calculated as

$$d_{inner} = \sqrt{\frac{4}{\pi} \cdot \frac{1{,}25P_{g\,max}}{i\sigma_{tear}}} \approx 1{,}26\sqrt{\frac{P_{g\,max}}{i\sigma_{tear}}}, \qquad (57)$$

where i is a number of studs;

σ_{tear} is an acceptable tearing stress (100-120 MPa).

The external diameter of the thread is interrelated with its internal diameter and a pitch t as

$$d_{ext} \approx d_{int} + 1.4 \cdot t. \qquad (58)$$

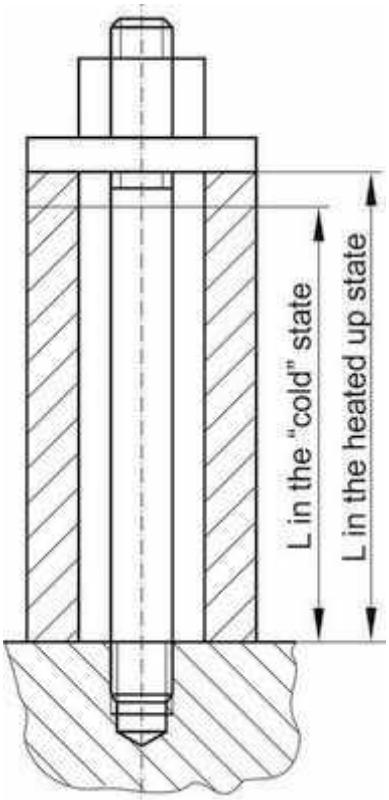

Figure 51 – For the stud strength analysis

The evaluated external diameter must be rounded up to the closest standard integer.

The diameter of the cylinder body usually matches the internal diameter of the thread.

The long power studs (like in the AM-38 engine), fastening cylinder block to the crankcase, are analyzed both on a breakaway and on a stresses that originate when the assembly is being heated (*Figure* 51). According to the power frame of the AM-38 engine (14 power studs per a six-cylinder block), the pretension of a single stud is equal to $(0.2-0.3)P_{g\,max}$ (the average value is $0.25 \cdot P_{g\,max}$). Then the corresponding tensile stress is

$$\sigma_{tens} \approx \frac{0.25 \cdot P_{g\,max}}{\frac{\pi d_{int}^2}{4}} = \frac{P_{g\,max}}{\pi d_{int}^2}, \qquad (59)$$

where d_{int} is a stud body diameter or inner diameter of the thread.

An additional temperature stress is evaluated according to the following algorithm:

1. The elongation of the aluminum block against the stud at a heated up

state is calculated as

$$\Delta L = L\left(\alpha_{alum}\Delta t_{cyl\ block} - \alpha_{steel}\Delta t_{stud}\right) \quad (60)$$

where L is a stud length or the length of the compressed block part;

α_{alum}, α_{steel} are the linear expansion coefficient of aluminum and steel;

$\Delta t_{cyl\ block}$, Δt_{stud} is an average temperature growth of the clock and the stud respectively (temperature difference between the cold and heated up engine).

2. It can be taken for the existing relations between the average rigidities of the studs the block that the relative change in length of the block and studs is 25 % absorbed in the form of barrel compression and 75 % - stud tension.

3. The stud elongation is evaluated as

$$\Delta L_{stud} \approx 0.75 \cdot \Delta L\,. \quad (61)$$

4. Finally, the additional temperature stress in the stud is

$$\sigma_{tens\ temp} = \frac{\Delta L_{stud}}{L} E, \quad (62)$$

where E is an elasticity modulus of the stud.

The total stress in the stud is evaluated as

$$\sigma_{tens\Sigma} = \sigma_{tens} + \sigma_{tens\ temp}. \quad (63)$$

The maximum acceptable total stress is 400 MPa.

27 SELF-MONITORING QUESTIONNAIRE

1. What loads act on the cylinders and cylinder blocks of the piston engines?
2. Name the power frames of the cylinders.
3. Name main parts and elements of the cylinder.
4. How is temperature distributed in the cylinder and the cylinder head during engine operation?
5. The shapes of the combustion chambers and their effect on an indicated efficiency.
6. The specific features of the cylinder and cylinder head cooling in the liquid-cooled and air-cooled engines.
7. What are the specific features of gas seam sealing?

8. Materials used for cylinders, cylinder heads and cylinder blocks.
9. Main approaches to strength analysis of the cylinder block parts.

28 REPORTING

In the theoretical part of the report you must briefly note all the chapters of this manual:

- an overview of the construction;
- examples of some constructions;
- materials and production aspects.

The report must also contain *Figure 35, 36, 38, 40, 43, 45*.

The special attention must be paid to materials and production aspects.

Before reporting you must get familiar with the mockups in the hall and in the 107 room of motor building, analyze the specific features of cylinders and their blocks. The results must be presented in a tabular format, as it is shown below.

Engine name and type	Power frame of a cylinder assembly: cylinder – cylinder head – cylinder block	Engine cooling	Construction of the combustion chamber

REFERENCES

1. Масленников, М. М. Авиационные поршневые двигатели [Текст] / М. М. Масленников, М. С. Рапипорт. – М. : Оборонгиз, 1951. – 847 с.

2. Двигатели внутреннего сгорания. Конструирование и расчет на прочность поршневых и комбинированных двигателей. [Текст] / Д. Н. Вырубов, С. И. Ефимов, Н. А. Иващенко [и др.]. ; под ред. А. С. Орлина, М. Г. Круглова. – М. : Машиностроение, 1984. – 384 с.

3. Луканин, В. Н. Двигатели внутреннего сгорания. Динамика и конструирование [Текст] / В. Н. Луканин, М. Г. Шатров. – М. : Высш. шк., 2005. – 400 с.

4. Авиационный мотор АШ-82ФН : описание конструкции [Текст]. – М. : Книга по требованию, 2012. – 129 с.

5. Заикин, А. Е. Авиационные двигатели. Конструкция и расчет деталей [Текст] / А. Е. Заикин. – М. : Оборонгиз. - 612 с.

6. Конструирование двигателей внутреннего сгорания: учеб. для вузов [Текст] / Н. Д. Чайнов, Н. А. Иващенко, А. Н. Краснокутский [и др.] ; под. ред. Н. Д. Чайнова. – М. : Машиностроение, 2008. – 496 с.

7. Конструкция авиационных двигателей [Текст] / А. В. Штода, С. П. Алешенко, А. Я. Иванов [и др.]. – М. : ВВИА им. проф. Н. Е. Жуковского, 1970. – Ч. 2. – 312 с.

Навчальне видання

Білогуб Олександр Віталійович
Гусєв Юрій Олексійович
Сіренко Фелікс Феліксович

ШАТУНИ, КОЛІНЧАСТІ ВАЛИ, ЦИЛІНДРИ І БЛОКИ АВІАЦІЙНИХ ПОРШНЕВИХ ДВИГУНІВ

(Англійською мовою)

Редактор О. В. Галкін
Технічний редактор Л. О. Кузьменко

Зв. план, 2017
Підписано до друку 24.03.2017
Формат 60х84 1/16. Папір офс. №2. Офс. друк
Ум. друк. арк. 4,2. Обл.- вид. арк. 4,75. Наклад 50 пр.
Замовлення 87 . Ціна вільна

Видавець і виготовлювач
Національний аерокосмічний університет ім. М. Є. Жуковського
«Харківський авіаційний інститут»
61070, Харків-70, вул. Чкалова, 17
http://www.khai.edu
Видавничий центр «ХАІ»
61070, Харків-70, вул.Чкалова,17
izdat@ khai.edu

Свідоцтво про внесення суб'єкта видавничої справи
до Державного реєстру видавців, виготовлювачів і розповсюджувачів
видавничої продукції сер. ДК № 391 від 30.03.2001